Direct reprogramming of fibroblasts into endothelial cells capable of angiogenesis and reendothelialization in tissue-engineered vessels

Andriana Margariti[a], Bernhard Winkler[a], Eirini Karamariti[a], Anna Zampetaki[a], Tsung-neng Tsai[a], Dilair Baban[b], Jiannis Ragoussis[b], Yi Huang[c], Jing-Dong J. Han[c], Lingfang Zeng[a], Yanhua Hu[a], and Qingbo Xu[a,1]

[a]Cardiovascular Division, King's College London British Heart Foundation Centre, London SE5 9NU, United Kingdom; [b]The Genomics Group, Welcome Trust Centre for Human Genetics, University of Oxford, Oxford OX3 7BN, United Kingdom; and [c]Chinese Academy of Sciences Key Laboratory of Computational Biology, Max Planck Partner Institute for Computational Biology, Shanghai Institutes for Biological Sciences, Shanghai 200031, China

Edited* by Shu Chien, University of California at San Diego, La Jolla, CA, and approved July 13, 2012 (received for review April 3, 2012)

The generation of induced pluripotent stem (iPS) cells is an important tool for regenerative medicine. However, the main restriction is the risk of tumor development. In this study we found that during the early stages of somatic cell reprogramming toward a pluripotent state, specific gene expression patterns are altered. Therefore, we developed a method to generate partial-iPS (PiPS) cells by transferring four reprogramming factors (OCT4, SOX2, KLF4, and c-MYC) to human fibroblasts for 4 d. PiPS cells did not form tumors in vivo and clearly displayed the potential to differentiate into endothelial cells (ECs) in response to defined media and culture conditions. To clarify the mechanism of PiPS cell differentiation into ECs, SET translocation (myeloid leukemia-associated) (SET) similar protein (SETSIP) was indentified to be induced during somatic cell reprogramming. Importantly, when PiPS cells were treated with VEGF, SETSIP was translocated to the cell nucleus, directly bound to the VE-cadherin promoter, increasing vascular endothelial-cadherin (VE-cadherin) expression levels and EC differentiation. Functionally, PiPS-ECs improved neovascularization and blood flow recovery in a hindlimb ischemic model. Furthermore, PiPS-ECs displayed good attachment, stabilization, patency, and typical vascular structure when seeded on decellularized vessel scaffolds. These findings indicate that reprogramming of fibroblasts into ECs via SETSIP and VEGF has a potential clinical application.

shear stress | stem cell therapy | vascular tissue engineering

An interesting aspect of research today is focused on the generation of functional cells to be used for regenerative medicine. For example, the damaged endothelial cells (ECs) on the vessel wall could be replaced by using EC-based therapy. The discovery of reprogramming induced pluripotent stem (iPS) cells from somatic cells (1–3) could pave the way for major advances in regenerative medicine. In comparison with embryonic stem cells, they could offer a tool for clinical application that does not raise either ethical or alloimmune concerns. iPS cell generation is mainly based on the sufficient delivery of a combination of key transcription factors, such as c-Myc, Klf4, Oct4, and Sox2 (2), or Lin28 and Nanog (4), which initiates the reprogramming of somatic cells into a pluripotent state. Methods have now been developed to drive the reprogramming factors in a way that overcomes the lentiviral vectors that stably integrated into the host cell genome (2, 5, 6). These methods include nonintegrating adenoviral vectors (7) and plasmids (8, 9), or delivery of the reprogramming factors as purified recombinant proteins (10) and modified RNA molecules (11–13).

iPS cells have displayed the potential to differentiate into a number of cell lineages, such as $CD34^+$ progenitor cells (14), cardiomyocytes (15, 16), and ECs (17). However, the main limitation for iPS cell application is the risk of tumor development, because these cells are reprogrammed to a fully pluripotent state. On the basis of the fact that cell reprogramming is a process with low efficiency, it is also possible that different stages of cell reprogramming may regulate signal pathways able to direct the differentiation of reprogrammed cells before the pluripotent state. Therefore, "skipping pluripotency" is a way to convert a somatic cell from one type to another. In this study we have established a method to generate partially induced pluripotent stem (PiPS) cells. This method includes transferring of the genes encoding the four transcription factors (OCT4, SOX2, KLF4, and c-MYC) to human fibroblasts, and culture in reprogramming media for 4 d. PiPS cells did not form tumors in vivo and had the potential to differentiate into ECs in response to defined media and culture conditions. We demonstrated that these PiPS cell-derived ECs are functional in angiogenesis in infarcted tissues in ischemic limb and in reendothelialization in tissue-engineered vessels ex vivo.

Results

Alterations of Gene Expression During Fibroblast Cell Reprogramming as Early as Day 4. Human fibroblasts were virally transduced with genes encoding the four transcription factors OCT4, SOX2, KLF4, and c-MYC, cultured in reprogramming media for 4, 7, 14, and 21 d, and subjected to microarray analysis. The results revealed that 198 genes were altered at day 4, 107 genes at day 7, 97 genes at day 14, and 131 genes at day 21 compared with day 0. Interestingly, when functional classification of the differentially expressed genes was performed using Ingenuity Systems software, significant differences observed in the expression of genes involved in cellular movement, cell death, cellular growth, proliferation, and development demonstrated that a high number of changes in the expression profile occur during early stages of reprogramming (4 d) compared with days 7, 14, and 21 (*SI Appendix*, Fig. S1, and Tables S2–S5). Importantly, a high number of genes mainly associated with vascular lineages, such as TEK, NRARP, STMN2, and filamin were also identified as differentially expressed in the microarray and confirmed by real-time PCR (Fig. 1 *A–D*). These results demonstrate that during somatic cell reprogramming toward a pluripotent state, specific gene expression patterns are altered as early as day 4.

Characterization of 4-d PiPS Cells. Human fibroblasts were reprogrammed for 4 d by nucleofecting with a linearized pCAG2LMKOSimO plasmid encoding the four genes defined as

Author contributions: A.M. and Q.X. designed research; A.M., B.W., E.K., A.Z., T.-n.T., D.B., J.R., Y. Huang, J.-D.J.H., and Y. Hu performed research; A.M., B.W., E.K., A.Z., D.B., J.R., Y. Huang, J.-D.J.H., L.Z., Y. Hu, and Q.X. analyzed data; and A.M., L.Z., Y. Hu, and Q.X. wrote the paper.

The authors declare no conflict of interest.

*This Direct Submission article had a prearranged editor.

Freely available online through the PNAS open access option.

[1]To whom correspondence should be addressed. E-mail: qingbo.xu@kcl.ac.uk.

This article contains supporting information online at www.pnas.org/lookup/suppl/doi:10.1073/pnas.1205526109/-/DCSupplemental.

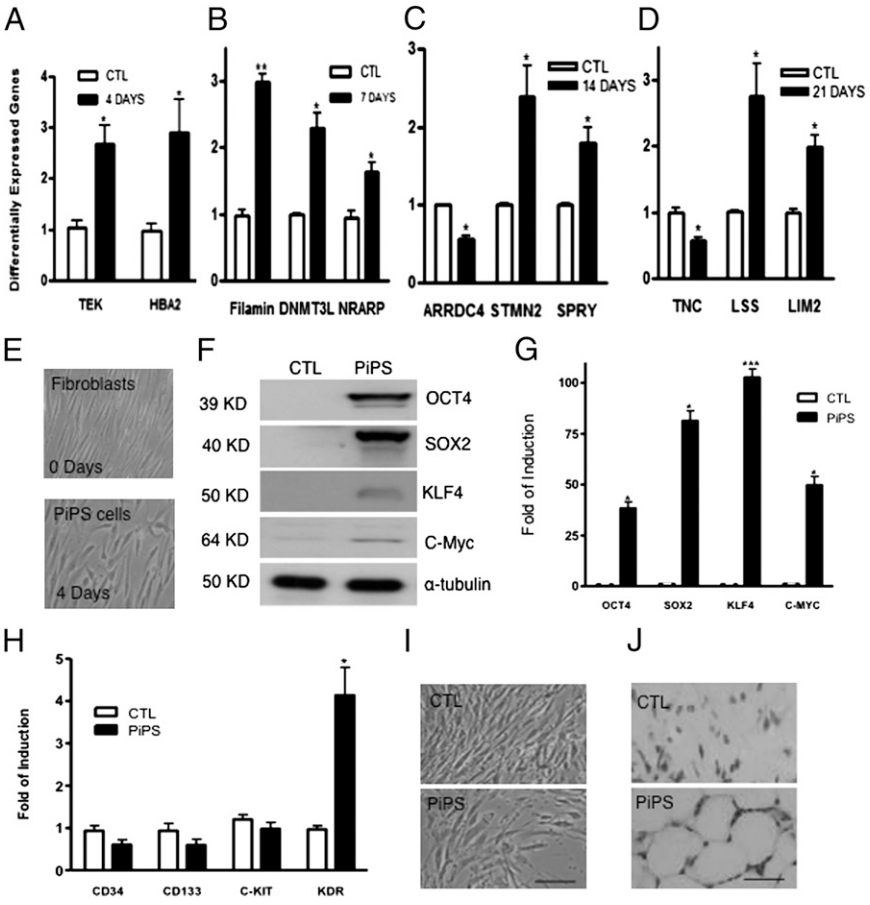

Fig. 1. Different expression of genes during reprogramming and characterization of 4-day PiPS cells. Differential expression profile of genes altered according to microarray analysis during reprogramming was confirmed by real-time PCR assays on day 4 (*A*), day 7 (*B*), day 14 (*C*), and day 21 (*D*) [data are means ± SEM ($n = 3$); $*P < 0.05$, $**P < 0.01$]. Human fibroblasts were nucleofected with a linearized pCAG2LMKOSimO plasmid encoding the four reprogramming genes (OCT4, SOX2, KLF4, and C-MYC) or an empty vector. Images show the morphology of fibroblasts, 4-day PiPS cells (*E*). PiPS cells expressed the four reprogramming factors at protein (*F*) and mRNA levels (*G*) [data are means ± SEM ($n = 3$); $*P < 0.05$, $***P < 0.001$]. (*H*) Real-time PCR assays for progenitor markers CD34, CD133, c-Kit, and KDR (VEGFR2) [data are means ± SEM ($n = 3$); $*P < 0.05$]. (*I*) PiPS cells were negative for alkaline phosphatase, whereas they formed capillary-like structures in in vivo Matrigel plug assays, when injected to SCID mice for 2 wk (*J*). (Scale bar, 50 μm.)

PiPS cells. PiPS cells displayed an alternate morphology distinct from the fibroblasts and did not form colonies in this early stage of reprogramming (Fig. 1*E*). PiPS cells expressed the four reprogramming factors at the protein (Fig. 1*F*) and mRNA levels (Fig. 1*G*). They showed an induced expression of VEGF receptor 2 (VEGFR2), kinase insert domain receptor (KDR) compared with the control, but not for the progenitor markers such as CD34, CD133, and c-Kit (Fig. 1*H*). PiPS cells were negative for alkaline phosphatase (Fig. 1*I*) and pluripotent markers such as SSEA-1 and TRA 1-81 and did not form tumors in vivo 2 mo after s.c. injection in SCID mice (*SI Appendix*, Fig. S2). In parallel, fully reprogrammed iPS cells were s.c. injected in SCID mice, where tumors were observed (*SI Appendix*, Fig. S2). Importantly, PiPS cells formed capillary-like structures in in vivo Matrigel plug assays in SCID mice, as revealed by H&E staining (Fig. 1*J*).

PiPS Cells Display the Potential to Differentiate into ECs. Because PiPS cells expressed VEGFR2, we wondered whether they can differentiate into vascular lineages and specifically into ECs. We found that PiPS cells from day 3 under the culture conditions start expressing EC markers, whereas high expression was detected up to day 9 (*SI Appendix*, Fig. S3). PiPS cells displayed an endothelial-like morphology in comparison with control cells on day 6 (Fig. 2*A*) and expressed endothelial-specific markers such as CD31, CD144, VEGFR2, eNOS, and vWF at mRNA (Fig. 2*B*) and protein levels (Fig. 2*C*). Immunofluorescence staining also revealed a typical endothelial staining for CD144 (Fig. 2*D*). FACS analysis confirmed expression of CD31 and CD144 (Fig. 2*E*) for PiPS-ECs, whereas undifferentiated PiPS cells were negative for CD31 (*SI Appendix*, Fig. S4*A*). PiPS cells were also tested for pluripotent markers, which were not expressed as FACS and real-time PCR analyses revealed (*SI Appendix*, Fig. S4 *B* and *C*). Moreover, the differentiated ECs were able to form vascular-like tubes in vitro (Fig. 2*F*) and in vivo (Fig. 2*G*, *Upper*) in Matrigel plugs. To distinguish from the endogenous ECs, the differentiated cells were labeled with Vybrant (red) before s.c. injection to SCID mice. As shown in Fig. 2*G* (*Lower*), Vybrant staining confirmed the contribution of the exogenous human cells to form tube-like structures in SCID mice. Further experiments indicated double staining of the cells with Vybrant and CD31 (Fig. 2*H*). These results suggest that PiPS cells can differentiate into ECs. We defined these cells as PiPS-ECs.

SET Translocation (Myeloid Leukemia-Associated) (SET) Similar Protein (SETSIP) Is Involved in Differentiation of PiPS-ECs. To shed light on the mechanisms involved in PiPS-ECs differentiation, a number of genes indentified from microarray analysis were screened. A gene defined as "similar to SET translocation protein" (SETSIP) was studied. SETSIP gives rise to a protein containing 10 additional amino acids in the N terminus (*SI Appendix*, Fig. S5*A*) in comparison with the known SET protein (*SI Appendix*, Fig. S5*B*). In our PiPS cell model, we found that SETSIP was expressed in parallel with endothelial markers (Fig. 3*A*) at mRNA and protein levels (Fig. 3*B*, *Left*, and quantification, *Right*). Additional experiments also indicated that VEGF further induced SETSIP expression at the protein level (*SI Appendix*, Fig. S6). Interestingly, down-regulation of SETSIP by shRNA in control and PIPS-ECs resulted in suppression of endothelial marker expression at protein (Fig. 3*C*) and mRNA levels on day 6 (Fig. 3*D*). Moreover, SETSIP overexpression in PiPS-ECs induced EC marker expression in mRNA (Fig. 3*E*) and proteins (Fig. 3*F*, *Left*, and quantification, *Right*). Importantly, SETSIP was translocated to the cell nucleus during PiPS-EC differentiation (Fig. 3*G*). To elucidate the underlying mechanism of the EC regulation by SETSIP, luciferase

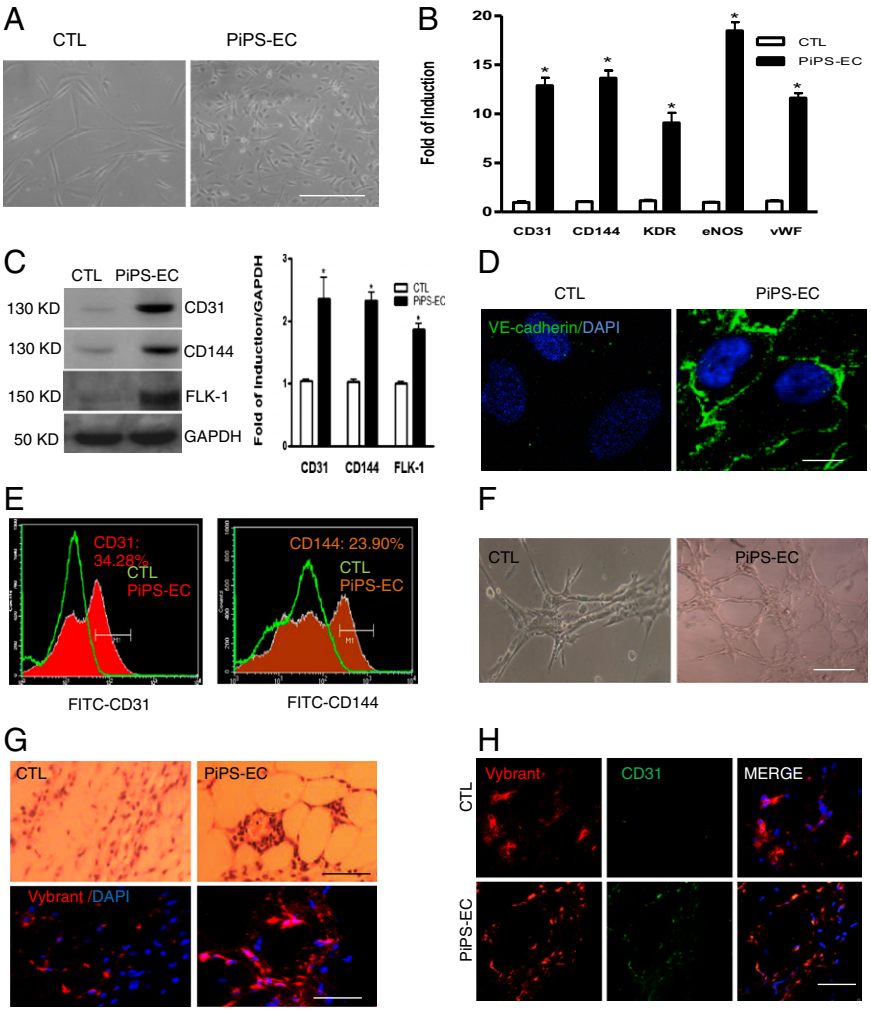

Fig. 2. PiPS cells differentiate into ECs. PiPS or control cells were seeded on collagen IV-coated plates and cultured with endothelial cell growth medium-2 (EGM-2) for 6 d. (*A*) Images show an endothelial-like morphology for PiPS-ECs in comparison with control cells, and expressed endothelial-specific cell markers, such as CD31, CD144, KDR, eNOS, and vWF, at the mRNA [data are means ± SEM ($n = 3$); $^*P < 0.05$] (*B*) and protein levels and quantification (*C*). (*D*) Immunoflurorescence staining showed a typical endothelial staining for CD144, and DAPI was used and stained the cell nucleus. (Scale bar, 25 μm.) (*E*) FACS analysis confirmed expression of CD31 and CD144. Representative images show vascular-like tubes in vitro (*F*) and in vivo (*G*, *Upper*) in Matrigel plug assays. PiPS-ECs labeled with Vybrant (red) before the s.c. injection in SCID mice (*G*, *Lower*) confirmed the presence of labeled human cells 2 wk later. The PiPS-ECs stained positive for Vybrant and CD31, whereas the control cells were positive only for the Vybrant but not for CD31 (*H*). (Scale bar, 50 μm.)

assays demonstrated that SETSIP induced the promoter activity of vascular endothelial-cadherin (VE-cadherin) (Fig. 3*H*). Moreover, ChIP assays confirmed these findings by showing a direct binding of SETSIP to the VE-cadherin gene promoter at region −864 to −1152 nt upstream of the transcription initiation site (Fig. 3*I*). These results indicate that SETSIP is important in PiPS-ECs differentiation. To answer questions such as how SETSIP is activated during cell reprogramming, examination of the SETSIP promoter binding sites predicts a possible binding with OCT1. To verify whether OCT1 is involved in the OCT4 signal pathway, further experiments revealed that OCT1 expression is induced during the early stages of reprogramming (*SI Appendix*, Fig. S7*A*), whereas overexpression of OCT4 in fibroblasts resulted in OCT1 and SETSIP activation (*SI Appendix*, Fig. S7*B*).

Establishing PiPS Cell Lines That Differentiate into EC Cells. To improve the purity of PiPS cells, human fibroblasts were nucleofected with the pCAG2LMKOSimO plasmid, which contains a neomycin resistant gene and an mOrange marker. PiPS cells were selected by neomycin treatment for 4 d, and a pure population of PiPS cells was obtained expressing the mOrange marker (*SI Appendix*, Fig. S8*A*) and the four genes (*SI Appendix*, Fig. S8*B*). The pure population of PiPS cells was subjected to differentiation and confirmed the potential of these cells to differentiate into the EC lineage, expressing endothelial markers (*SI Appendix*, Fig. S8*C*). Moreover, PiPS-EC–derived cells displayed the capacity of low-density lipoprotein uptake (*SI Appendix*, Fig. S8*D*). Importantly, luciferase assays demonstrated that PiPS-ECs derived from a pure population of PiPS cells had an increased promoter activity of VE-cadherin compared with control cells (*SI Appendix*, Fig. S8*E*). Additional experiments revealed that knockdown of SETSIP by shRNA in PiPS-ECs after selection resulted in suppression of VE-cadherin at the protein level (*SI Appendix*, Fig. S8*F*). Luciferase assays also showed that knockdown of SETSIP decreased the VE-cadherin promoter activity in PiPS-ECs (*SI Appendix*, Fig. S8*G*). Furthermore, knockdown of SETSIP in PiPS-ECs by shRNA abolished the formation of vascular-like tubes in vivo in Matrigel plugs (*SI Appendix*, Fig. S8*H*). These results support the notion that SETSIP has an important role in PiPS-EC differentiation derived from a pure population of PiPS cells.

PiPS-ECs Display Endothelial Properties in Vivo. Functionally, PiPS-ECs promoted significantly higher blood flow compared with fibroblasts when injected i.m. into an ischemic model of SCID mice (Fig. 4*A*). They showed significantly increased blood flow compared with control (no cells) and fibroblasts (Fig. 4*B*). PiPS-ECs also displayed significantly higher capillary numbers in comparison with fibroblasts (Fig. 4 *C* and *D*) when staining with CD31 antibody. Engrafted PiPS-ECs displayed a typical vascular architecture, whereas in the control experiments the injected fibroblasts were present in a random pattern, and no vascular structures were observed (Fig. 4*E*). Finally, when PiPS-ECs or fibroblasts were stained and quantified with a human specific CD31 antibody, PiPS-ECs displayed an enhanced engraftment ability (Fig. 4 *E* and *F*). In addition, PiPS-ECs showed the ability to participate in tissue regeneration when they were seeded on decellularized vessel

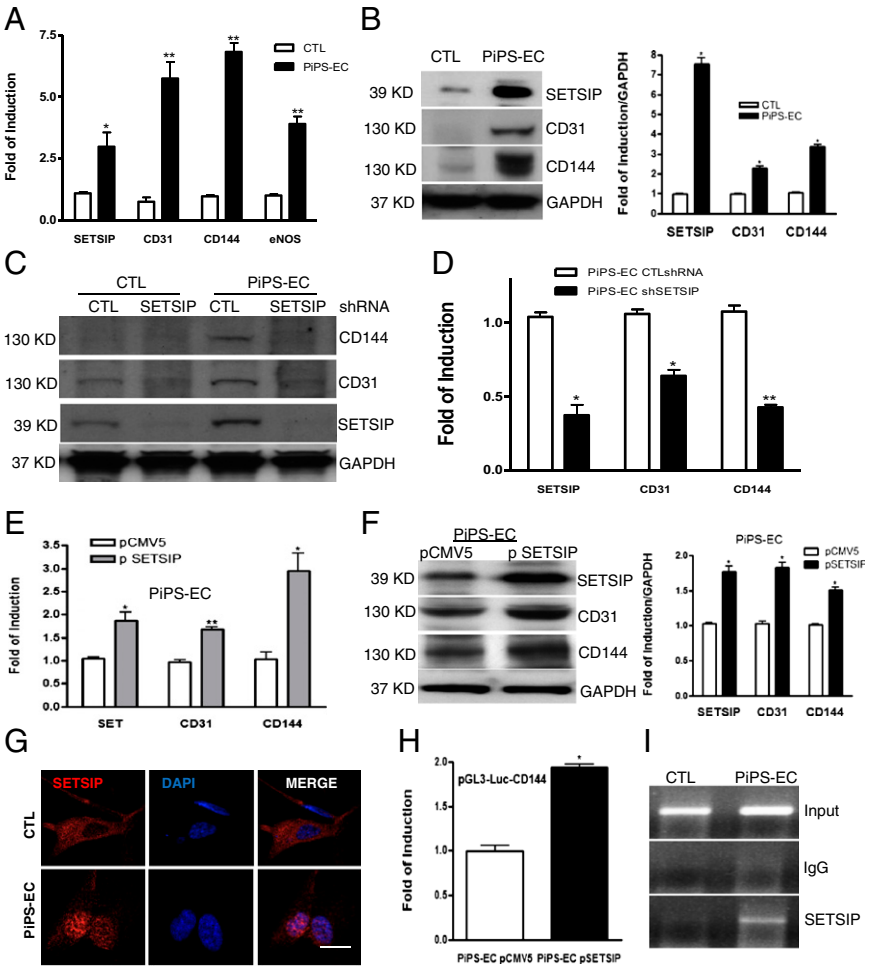

Fig. 3. SETSIP is involved in differentiation of PiPS-ECs. Real-time PCR shows SETSIP parallel expression with EC markers at the mRNA [*A*; data are means ± SEM ($n = 3$); $^*P < 0.05$, $^{**}P < 0.01$] and protein (*B*) levels and quantification (*Right*), in PiPS-ECs at day 6 of differentiation. SETSIP was knocked down by shRNA in CTL and PiPS-ECs at day 3 of differentiation, showing a suppression in endothelial markers assessed on day 6 at protein (*C*) and mRNA levels [*D*; data are means ± SEM ($n = 3$); $^*P < 0.05$, $^{**}P < 0.01$]. SETSIP overexpression using pCMV5-SETSIP construct (p SETSIP) or empty vector pCMV5 in PiPS-ECs during EC differentiation at day 4, showing further induction in EC marker expression at mRNA [*E*; data are means ± SEM ($n = 3$); $^*P < 0.05$, $^{**}P < 0.01$] and protein levels, and quantification (*F*), when assessed at day 6. Immunostaining shows translocation of SETSIP to the cell nucleus during PiPS-ECs differentiation at day 6; DAPI was used and stained the cell nucleus (*G*). (Scale bar, 50 μm.) Luciferase assays were performed at day 4 during PiPS-ECs differentiation, showing an increased promoter activity for VE-cadherin in the presence of the SETSIP at day 6 of differentiation (*H*; data are means ± SEM ($n = 3$); $^*P < 0.05$]. ChIP assays revealed that SETSIP binds directly to the VE-cadherin gene promoter at region (−864 to −1152) nt upstream of the transcription initiation site in 6-day differentiated PiPS-ECs (*I*).

scaffolds in a specially constructed bioreactor and harvested on day 5. Ex vivo the PiPS-ECs seeded vessels were fixed and stained positive for endothelial markers CD31 (Fig. 5*A*) and CD144 (Fig. 5*B*), demonstrating a highly elongated and oriented pattern. Such staining was not obtained for control fibroblasts (Fig. 5 *A* and *B*). Importantly, in the ex vivo bioreactor, the PiPS-ECs seeded scaffolds displayed normal vessel morphology, whereas the lumen was almost blocked in some of the fibroblast-seeded vessels (Fig. 5*C*). These results indicate that PiPS-ECs display endothelial functions when tested ex vivo. To test whether PiPS cells have an ability to directly differentiate into vascular lineage such as smooth-muscle cells and EC ex vivo, the reendothelialization potential of PiPS cells in tissue-engineered vessels was assessed. The vessels were sectioned and stained with H&E (Fig. 5*D*). The double-seeded scaffolds with PiPS cells showed a native vessel architecture with multiple layers of smooth-muscle cells while an EC layer was present (Fig. 5 *D* and *E*). The multiple layers of cells increased vessel wall stability and integrity to a high level, matching results of native nondecellularized aortic grafts (Fig. 5*D*). The double-seeded PiPS cell-derived vessels were fixed and stained positive for endothelial markers such as CD31 (Fig. 5*F*) and CD144 (Fig. 5*G*) and for smooth-muscle markers such as SMA (Fig. 5 *F* and *G*, *Left* panel) and SM22 (Fig. 5 *F* and *G*, *Right*).

Discussion

iPS cell generation is a fascinating tool for regenerative medicine that provides the potential to create patient-specific cells to be used in cell-based therapies. Although important technical progress has been made in iPS cell generation (3, 8, 11, 13, 18) from a number of somatic cell sources, iPS cell research is still in its initial stages. Various issues need to be addressed regarding iPS safety and reprogramming mechanisms. In this study, we developed a method to generate a population of PiPS cells from human fibroblasts through short-term reprogramming and selection. We found that during somatic cell reprogramming the expression of genes involved in cell differentiation into specific cell lineages was altered as early as day 4. PiPS cells displayed the ability to differentiate into ECs through defined media and culture conditions by "skipping pluripotency" without tumor risk. In line with our findings, recent studies have reported the direct conversion of human fibroblasts to blood progenitors (19), germ cells into neurons (20), conversion of mouse and human fibroblasts into functional spinal motor neurons (21), and conversion of mouse fibroblasts into cardiomyocytes by defined factors (22) or using a direct reprogramming strategy (23).

During reprogramming the genome of a somatic cell is entering a process to reach pluripotency. Interestingly, microarray analysis revealed that during the early stages of reprogramming, a number of signal pathways involved in cell-specific lineage differentiation were changed. For example, the expression of genes related to differentiation of connective tissue, muscle cell lines, adipocytes, bone cell, mononuclear cells, osteoclast-like cells, or even adhesion of ECs were altered as early as day 4. Moreover, the induction of genes such as DNA (cytosine-5-)-methyltransferase 3-like (DNMT3L) from day 7 of cell reprogramming, sustains the notion that the above signal pathways may be supported by genome-wide adjustments of repressive and active epigenetic features such as DNA methylation and histone

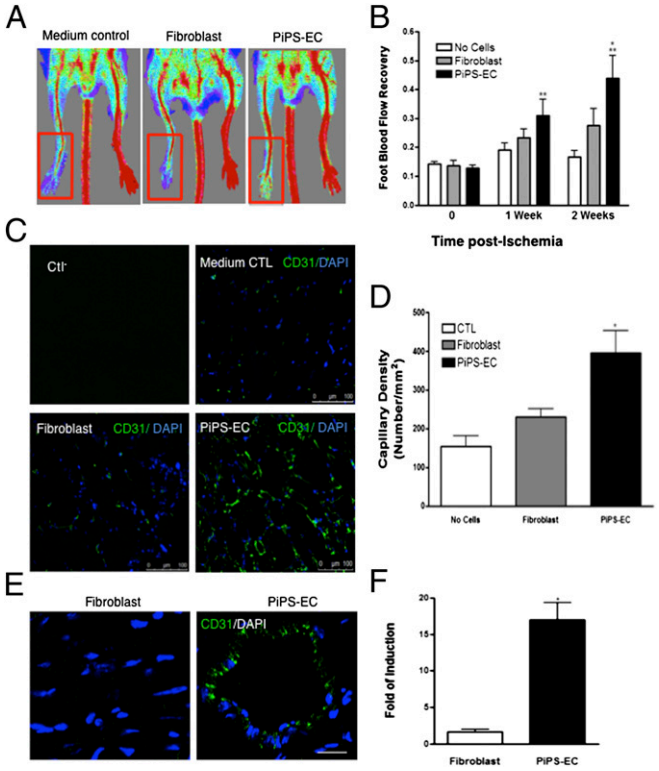

Fig. 4. PiPS-ECs improved neovascularization and blood flow recovery in a hindlimb ischemic model. PiPS-ECs, fibroblasts, or medium control (no cells) were injected i.m. into adductors of an ischemic model of SCID mice. (*A*) Representative color laser Doppler images of superficial blood flow (BF) in lower limbs taken 2 wk after ischemia induction. (*B*) Line graph shows the time course of postischemic foot BF recovery (calculated as the ratio between ischemic foot BF and contralateral foot BF) in mice given medium as control, fibroblasts, and PiPS-ECs. Statistical analysis showed significantly higher foot BF recovery for PiPS-ECs in comparison with both "no cells" control and fibroblasts at weeks 1 and 2 [data are means ± SEM ($n = 6$)]. Week 1: $^{**}P < 0.01$, PiPS-EC vs. "no cells" control; $^{**}P < 0.01$, PiPS-EC vs. fibroblasts. Week 2: $^{**}P < 0.01$, PiPS-EC vs "no cell" control; $^{*}P < 0.05$ PiPS-EC vs. fibroblasts. No significant differences were detected when fibroblasts were compared with "no cells" control. (*C*) Sections of adductors muscles were stained with CD31 antibody, and capillary density was expressed as the capillary number per mm^2 [*D*; data are means ± SEM ($n = 3$); $^{*}P < 0.05$]. (Scale bar, 100 μm.) (*E*) PiPS-ECs displayed an enhanced engraftment ability compared with fibroblasts when stained and quantified with a human-specific CD31 antibody at six randomly selected microscopic fields (at ×100) [*F*; data are means ± SEM ($n = 3$); $^{*}P < 0.05$]. (Scale bar, 50 μm.)

modifications, which change the chromatin remodeling complexes (24–26). Additionally, during the later stages of reprogramming, such as days 14 and 21, more signal pathways linked with cell lineage differentiation were identified to display differential gene expression profiles. Therefore, PiPS cells are in a transient state that is able to undergo direct differentiation in response to specific stimulus, such as the expression of lineage-specific factors.

VEGF has been shown to be the first secreted molecule with specificity for the endothelium during development (27). Cells that respond to VEGF must first express its receptors (VEGFR1 and VEGFR2 or KDR). KDR, which forms a complex with VE-cadherin, β-catenin, and PI3-K (28), is the earliest marker for the endothelial lineage during development. In our PiPS cell model high KDR expression was detected, suggesting that these cells may be responsive to VEGF stimulation and thus capable of differentiation to ECs. Furthermore, SET (29) is a multitasking protein that is involved in apoptosis, transcription, differentiation, nucleosome assembly, and histone binding. In our study we found that when reprogrammed cells were stimulated with VEGF, EC differentiation was induced, and SETSIP was translocated to the cell nucleus. SETSIP was binding to the VE-cadherin gene promoter, resulting in increased VE-cadherin gene expression. Further experiments have shown that SETSIP is expressed in mature ECs in comparable levels to PiPS-ECs (*SI Appendix*, Fig. S9 *A* and *B*). Interestingly, in both mature ECs and PiPS-ECs SETSIP is localized in the nucleus (*SI Appendix*, Fig. S9*A*). Therefore, SETSIP through regulation of VE-cadherin has an important role in the functional properties of ECs. Our results demonstrate that EC differentiation is induced through the OCT4-SETSIP and VEGF pathway and link the cell reprogramming of fibroblasts with the directed differentiation to EC cells.

The present findings of PiPS cells-derived ECs that expressed a panel of endothelial markers at mRNA and protein levels and formed vascular-like tubes in vitro and in vivo have several implications. First, the time from reprogramming to obtaining ECs is less than 2 wk, which makes this protocol feasible for treatment of patients with a personalized cell therapy (e.g., leg ischemia). In this study three human fibroblast cell lines have been reprogrammed and differentiated to ECs, achieving comparable results. However, we should point out that it has not been tested with fibroblasts from patients. Second, one of the main concerns of stem cell

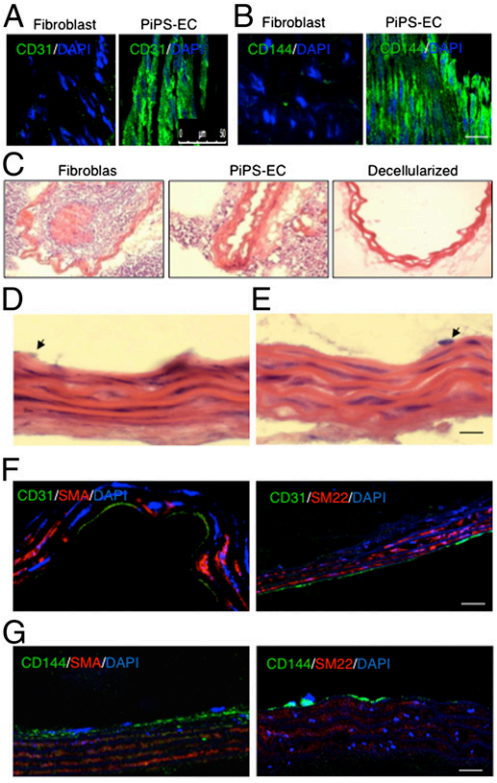

Fig. 5. PiPS-ECs displayed endothelial properties ex vivo. PiPS-ECs or fibroblasts were seeded on decellularized vessel scaffolds in a specially constructed bioreactor and harvested on day 5. (*A* and *B*) En face positive staining for endothelial markers CD31 and CD144 is shown in the PiPS-EC. (Scale bar, 50 μm.) (*C*) H&E staining showed that fibroblast-seeded vessels were almost occluded, whereas PiPS-ECs-seeded scaffolds presented with a normal vessel morphology. (*D* and *E*) Cross-sections with H&E staining of the double-seeded scaffolds with selected PiPS cells, which were induced to be differentiated into smooth-muscle cells and ECs, showing a native-like vessel architecture with multiple layers of smooth-muscle cells and a monolayer of ECs. Arrows indicate an endothelial-like cell. (*F* and *G*) Double-seeded PiPS cell-derived vessels were fixed and stained positive for EC markers, such as CD31 and CD144, and for smooth-muscle markers, such as SMA and SM22. (Scale bar, 50 μm.)

therapy, tumor formation, is eliminated,and the purity of the autologous cells used is no longer an issue because PiPS cells do not develop teratomas in SCID mice. In addition, even if the efficiency of human fibroblast transfected with the four reprogramming factors (using a single plasmid by nucleofection) was ~30%, the purity of PiPS cells is not an issue because a pure population of PiPS cells can be selected and further differentiated into ECs. Importantly, PiPS-ECs functionally displayed good attachment, stabilization, patency, and typical endothelial structure [e.g., formation of adhesion junction (CD144) in animal models]. When they were used for preparation of tissue-engineered vessels, the vessels displayed functional properties and showed better recovery of tissue blood flow when injected i.m. into ischemic legs in comparison with control fibroblasts. Finally, when a pure population of PiPS cells is used, tissue-engineered vessels show a native-vessel architecture, with multiple layers of smooth-muscle cells and an EC layer. Therefore, PiPS cells could be a valuable source for treatment of ischemic tissues and for generation of tissue-engineered blood vessels.

In summary, PiPS cells have the potential to differentiate into ECs in response to defined media and culture conditions. SETSIP was identified to be translocated to the cell nucleus and directly bound to the VE-cadherin promoter, inducing EC differentiation. Thus, we developed a method to generate PiPS cells from human fibroblasts through short-term reprogramming that can differentiate into ECs without tumor risk, via the OCT4-SETSIP and VEGF pathway (*SI Appendix*, Fig. S10). PiPS cells can be a useful cell source for regenerating damaged tissue and vascular tissue engineering ex vivo.

Materials and Methods

Cell Reprogramming. Fibroblasts were nucleofected with the four reprogrammed factors or control empty vector and cultured with reprogramming media composed of Knockout DMEM (Invitrogen, SKU-10829-018), 20% Knockout Serum Replacement (Invitrogen, SKU 10828-028), 10 ng/mL basic fibroblast growth factor (Miltenyi Biotec, 130-093-837), 0.1 mM β-mercaptoethanol, and 0.1 mM MEM nonessential amino acids. The media were changed every day. Procedure details are in *SI Appendix, SI Materials and Methods*.

SETSIP Cloning and Nucleofection. Full-length human SETSIP cDNA fragment was obtained by RT-PCR from PiPS-ECs with the primer set shown in *SI Appendix*, Table S2 and cloned into Kpn1 and Xba1 sites of a pCMV5 plasmid defined as pCMV5-SETSIP.

Selection of PiPS Cells. Fibroblasts were nucleofected with a polycistronic plasmid containing all four factors, OCT4, SOX2, KLF4, and C-MYC (OSKM), as shown above. Neomycin selection was started 1 d after the nucleofection up to day 4, when a pure population of PiPS cells has been obtained expressing an mOrange marker and the four reprogrammed genes.

Cell Seeding and Vascular Bioreactor. PiPS-ECs or fibroblasts were seeded on aortic grafts, which were previously decellularized (with SDS at 0.075% and washed in PBS), in a special constructed bioreactor, and shear stress was applied. Procedure details are in *SI Appendix, SI Materials and Methods*.

En Face Preparation and Immunofluoresence Staining and Frozen Section Staining. The procedure for en face preparation is similar to that described elsewhere (30).

Statistical Analysis. Data were analysis using GraphPad Prism Software. Data expressed as means ± SEM were analyzed with a two-tailed Student *t* test for two groups. A value of $P < 0.05$ was considered significant.

ACKNOWLEDGMENTS. This work was supported by grants from the British Heart Foundation, the Oak Foundation, Jubilaeumsstiftung Basel, Stem Cell Leading Project XDA01010303, and by Wellcome Trust Grant 075491/Z/04.

1. Takahashi K, Okita K, Nakagawa M, Yamanaka S (2007) Induction of pluripotent stem cells from fibroblast cultures. *Nat Protoc* 2:3081–3089.
2. Takahashi K, Yamanaka S (2006) Induction of pluripotent stem cells from mouse embryonic and adult fibroblast cultures by defined factors. *Cell* 126:663–676.
3. Okita K, Nakagawa M, Hyenjong H, Ichisaka T, Yamanaka S (2008) Generation of mouse induced pluripotent stem cells without viral vectors. *Science* 322:949–953.
4. Yu J, et al. (2007) Induced pluripotent stem cell lines derived from human somatic cells. *Science* 318:1917–1920.
5. Maherali N, et al. (2007) Directly reprogrammed fibroblasts show global epigenetic remodeling and widespread tissue contribution. *Cell Stem Cell* 1:55–70.
6. Okita K, Ichisaka T, Yamanaka S (2007) Generation of germline-competent induced pluripotent stem cells. *Nature* 448:313–317.
7. Stadtfeld M, Nagaya M, Utikal J, Weir G, Hochedlinger K (2008) Induced pluripotent stem cells generated without viral integration. *Science* 322:945–949.
8. Chang CW, et al. (2009) Polycistronic lentiviral vector for "hit and run" reprogramming of adult skin fibroblasts to induced pluripotent stem cells. *Stem Cells* 27: 1042–1049.
9. Sommer CA, et al. (2010) Excision of reprogramming transgenes improves the differentiation potential of iPS cells generated with a single excisable vector. *Stem Cells* 28:64–74.
10. Zhou H, et al. (2009) Generation of induced pluripotent stem cells using recombinant proteins. *Cell Stem Cell* 4:381–384.
11. Warren L, et al. (2010) Highly efficient reprogramming to pluripotency and directed differentiation of human cells with synthetic modified mRNA. *Cell Stem Cell* 7: 618–630.
12. Desponts C, Ding S (2010) Using small molecules to improve generation of induced pluripotent stem cells from somatic cells. *Methods Mol Biol* 636:207–218.
13. Li W, Ding S (2010) Small molecules that modulate embryonic stem cell fate and somatic cell reprogramming. *Trends Pharmacol Sci* 31:36–45.
14. Park SW, et al. (2010) Efficient differentiation of human pluripotent stem cells into functional CD34+ progenitor cells by combined modulation of the MEK/ERK and BMP4 signaling pathways. *Blood* 116:5762–5772.
15. Dambrot C, Passier R, Atsma D, Mummery CL (2011) Cardiomyocyte differentiation of pluripotent stem cells and their use as cardiac disease models. *Biochem J* 434:25–35.
16. Kattman SJ, et al. (2011) Stage-specific optimization of activin/nodal and BMP signaling promotes cardiac differentiation of mouse and human pluripotent stem cell lines. *Cell Stem Cell* 8:228–240.
17. Li Z, Hu S, Ghosh Z, Han Z, Wu JC (2011) Functional characterization and expression profiling of human induced pluripotent stem cell- and embryonic stem cell-derived endothelial cells. *Stem Cells Dev* 20:1701–1710.
18. Kaji K, et al. (2009) Virus-free induction of pluripotency and subsequent excision of reprogramming factors. *Nature* 458:771–775.
19. Szabo E, et al. (2010) Direct conversion of human fibroblasts to multilineage blood progenitors. *Nature* 468:521–526.
20. Tursun B, Patel T, Kratsios P, Hobert O (2011) Direct conversion of *C. elegans* germ cells into specific neuron types. *Science* 331:304–308.
21. Son EY, et al. (2011) Conversion of mouse and human fibroblasts into functional spinal motor neurons. *Cell Stem Cell* 9:205–218.
22. Ieda M, et al. (2010) Direct reprogramming of fibroblasts into functional cardiomyocytes by defined factors. *Cell* 142:375–386.
23. Efe JA, et al. (2011) Conversion of mouse fibroblasts into cardiomyocytes using a direct reprogramming strategy. *Nat Cell Biol* 13:215–222.
24. Jaenisch R, Young R (2008) Stem cells, the molecular circuitry of pluripotency and nuclear reprogramming. *Cell* 132:567–582.
25. Zhou Q, Melton DA (2008) Extreme makeover: converting one cell into another. *Cell Stem Cell* 3:382–388.
26. Welstead GG, Schorderet P, Boyer LA (2008) The reprogramming language of pluripotency. *Curr Opin Genet Dev* 18:123–129.
27. Carmeliet P, et al. (1996) Abnormal blood vessel development and lethality in embryos lacking a single VEGF allele. *Nature* 380:435–439.
28. Carmeliet P, et al. (1999) Targeted deficiency or cytosolic truncation of the VE-cadherin gene in mice impairs VEGF-mediated endothelial survival and angiogenesis. *Cell* 98:147–157.
29. Fan Z, Beresford PJ, Oh DY, Zhang D, Lieberman J (2003) Tumor suppressor NM23-H1 is a granzyme A-activated DNase during CTL-mediated apoptosis, and the nucleosome assembly protein SET is its inhibitor. *Cell* 112:659–672.
30. Zeng L, et al. (2009) Sustained activation of XBP1 splicing leads to endothelial apoptosis and atherosclerosis development in response to disturbed flow. *Proc Natl Acad Sci USA* 106:8326–8331.

Supporting Information

Margariti et al.

SI Methods and Materials

Materials. Antibodies: mouse anti-Oct4 (sc-5279), rabbit anti-Klf4 (sc-20691), rabbit anti- c-Myc (sc-789), goat anti-I2PP2A (E-15) (sc-5655), goat anti-CD31 (SC-31045), goat anti-VE-Cadherin (sc-6458), and rabbit anti-GAPDH (FL335, sc-25778) were purchased from Santa Cruz Biotech (Santa Cruz, CA, USA). Rabbit oct4 (abcam), rabbit Nanog (abcam), Rabbit anti-Sox2 (ab59776), rabbit anti-VE-Cadherin (FITC) ab33321, mouse anti-CD31 (FITC) (ab13466), rabbit anti-IgG- FITC, mouse anti-IgG isotype control (ab37359), rabbit IgG isotype control (abcam) rabbit anti-CD31 (ab32457) (human specific), rabbit anti-CD31 (ab28364), rabbit-anti-SM22 (ab14106) and anti-mouse FLK-1 (ab2349-500) were purchased from Abcam. Rabbit anti-VE-Cadherin (human specific, 2158) was from Cell Signaling. Mouse anti-human Nestin, Mouse anti-Neuron-specific β-III Tubulin, Mouse anti-Oligodendrocyte Marker O4, Goat anti-mouse FABP-4 (962643), Mouse anti-human Osteocalcin (962645), Goat anti-human Aggrecan (962644), and anti-hVEGF (R2/KDR, FAB357F) were from R&D Systems. Mouse TRA-1-60 and Mouse TRA-1-81 (Millipore). The anti-Actin α-smooth muscle cy3 (C6198) was from SIGMA. The secondary antibodies; anti-goat Alexa488, anti-goat Alexa594, and anti-rabbit Alexa488, anti-rabbit Alexa594 were purchased from Invitrogen. The secondary antibody anti-mouse FITC, anti-goat FITC were from Dakocytomation (Glostrup, Denmark). Geneticin G-418 Sulphate (11811-023) was purchased from GIBCO. Recombinant human VEGF and PDGF-BB was purchased from R&D Systems.

Cell culture. Three human fibroblast cell lines were used in this study; CCD-1079 Sk CRL-2097 from Skin newborn (ATCC), and CCL-186 from lung 16 weeks gestation IMR-90 (ATCC), CCL-153 (ATCC). Fibroblasts were cultured on gelatine coated flasks (0.04%, Sigma) in ATCC-formulated Eagle's Minimum Essential Medium, (30-2003, ATCC) supplemented with 10% fetal bovine serum (30-2020, ATCC) and 100IU/ml penicillin and streptomycin in a humidified incubator supplemented with 5% CO_2 at 37°C. The cells were passaged every 3 days at a ratio of 1:3 to 1:6 and the medium was refreshed every 2 days.

Cell reprogramming. Fibroblasts were nucleofected with the four reprogrammed factors or control empty vector and cultured with reprogramming media comprised of Knockout DMEM (Invitrogen, SKU-10829-018), 20% Knockout Serum Replacement (Invitrogen SKU 10828-028), 10ng/ml basic fibroblast growth factor (bFGF Miltenyi Biotec, 130-093-837), 0.1mM β-mercaptoethanol and 0.1mM MEM non essential amino acids (MEM NEAA). The media were changed every day.

Microarray analysis. For the microarray analysis, fibroblasts were infected with 4 lentiviral vectors (EX-Z0092-Lv08-OCT4, EX-Z2845-Lv08-v-Myc, EX-Q0453-Lv08-KLF4, EX-T2547-Lv08-SOX2) purchased from GeneCopoeia. An empty vector (Ex-Lv08) was used as control. Samples were collected on days 4, 7, 14 and 21, RNA was extracted and a microarray analysis was performed and compared to control groups. In Brief, total RNA was extracted from each sample using RNeasy Mini Kit from Qiagen. The RNA quantity was measured using a NanoDrop ND-1000 spectrophotometer (NanoDrop Technologies, Wilmington, DE), and RNA quality was checked using RNA6000 Nano Assay on Agilent BioAnalyzer 2100 (Agilent Technologies, Santa Clara, CA). Commercially available high-density oligonucleotide, from Illumina whole genome gene expression BeadChips (Human HT12_V3_0_R3_11283641, Illumina Inc, San Diego, California, USA), were used with 48803 probes representing 37879 human transcripts. In brief, 500ng of total RNAs were reverse transcribed to synthesize first- and second- strand complementary DNA (cDNA), followed by in vitro transcription to synthesize biotin-labeled complementary RNA (cRNA) using TotalPrep-96 RNA amplification kit from Ambion accordingly. A total of 750ng of biotin-labeled cRNA from each sample was hybridized to the HT12 BeadChip (Illumina Inc., San Diego, CA) at 58C for 18 h. The hybridized BeadChip was washed and labeled with streptavidin-Cy3 according to the manufacture protocols. Chips were scanned with Illumina BeadScan and scanned image was imported into GenomeStudioV2010.1 (Illumina Inc) for data extraction.

SETSIP cloning and nucleofection. Full length human SETSIP cDNA fragment was obtained by RT-PCR from PiPS-ECs with the primer set shown in Supplemental Table S1 and cloned into Kpn1 and Xba1 sites of a pCMV5 plasmid defined as pCMV5-SETSIP. The construct was verified by DNA

sequencing. pCMV5-SETSIP or pCMV5 have been overexpressed in PiPS-EC cells by nucleofection and the endothelial marker expression was tested in transcriptional and protein levels.

Selection of PiPS cells. Fibroblasts were nucleofected with a polycistronic plasmid (OSKM) containing all four factors as shown above. Neomycin selection was started one day after the nucleofection up to day four where a pure population of PiPS cells has been obtained expressing an mOrange marker and the four reprogrammed genes.

Cell differentiation. PiPS cells were seeded on mouse collagen IV (BD mouse collagen IV-5μg/ml)-coated flasks or plates in EGM-2 media (Lonza) to induce endothelial differentiation for indicated times. The medium was refreshed every other day. PiPS cells were also differentiated into neuron cells using R&D Systems Human Stem cell Neural Kit SC011 according to the protocol provided. PiPS cells were differentiated into adipocytes, osteocytes and chondrocytes based on R&D Systems Human Mesechymal Stem Cell Kit SC006 according to the protocol provided.

Reverse transcriptase-polymerase chain reaction (RT-PCR) and real-time PCR. RT-PCR and real time PCR were performed as described previously (1). Total RNA was extracted using the RNeasy Mini Kit (Qiagen) according to the manufacturer's protocol. 2 μg RNA were reversely transcribed into cDNA with random primer by MMLV reverse transcriptase (RT) (Promega). 20-50ng cDNA (relative to RNA amount) was amplified by standard PCR with *Taq* DNA polymerase (Invitrogen) or real time PCR. PCR primers were designed using Primer Express software (Applied Biosystems). The primers' sequences are shown in Supplementary Table S1.

Immunofluorescence staining. The procedure used for immunofluorescent staining was similar to that described previously (1). Briefly, cells were fixed with 4% paraformaldehyde and permeabilised with 0.1% Triton X-100 in PBS for 10 min and blocked in 5% swine serum in PBS for 30 min at 37˚C. The cells were incubated with primary antibodies: goat anti-VE-cadherin, goat anti-CD31, goat anti-I2PP2A, rabbit anti-CD31 (human specific), rabbit anti-VE-cadherin (human specific), rabbit anti-SM22, anti-Actin α-smooth muscle cy3, mouse Nestin, mouse anti-Neuron-specific β-III Tubulin, mouse anti-Oligodendrocyte, mouse anti- Osteocalcin, goat anti-FABP-4, and goat anti-Aggrecan. The bound primary antibodies were revealed by incubation with the secondary antibodies; anti-goat Alexa488, anti-goat Alexa594, anti-rabbit Alexa488, anti-rabbit Alexa594, anti-mouse FITC, anti-goat FITC at 37^{o}C for 30 min. Cells were counterstained with 4',6-diamidino-2-phenylindole (DAPI; Sigma), mounted in Floromount-G (Cytomation; DAKO, Glostrup, Denmark), and examined with a fluorescence microscope (Axioplan 2 imaging; Zeiss) or SP5 confocal microscope (Leica, Germany).

Immunoblotting. The method used was similar to that described previously (1). Cells were harvested and washed with cold PBS, re-suspended in lysis buffer (25mM Tris-Cl pH 7.5, 120mM NaCl, 1 mM EDTA pH 8.0, 0.5% Triton X100) supplemented with protease inhibitors (Roche) and lysed by ultra-sonication (twice, 6 seconds each) (Bradson Sonifier150) to obtain whole cell lysate. The protein concentration was determined using the Biorad Protein Assay Reagent. 50μg of whole lysate was applied to SDS-PAGE and transferred to Hybond PVDF membrane (GE Health), followed by standard western blot procedure. The bound primary antibodies were detected by the use of horseradish peroxidase (HRP)-conjugated secondary antibody and the ECL detection system (GE Health). The band density was semiquantified by Adobe Photoshop software.

Alkaline phosphatase staining. Alkaline phosphatase staining was conducted following the manufacturer's instructions (Vector blue Alkaline phosphatase kit III, Cat. No. SK-5300).

Teratoma formation assay. PiPS cells ($1x10^6$) were mixed with Matrigel and subcutaneously injected into SCID mice. Eight weeks later, the plugs were harvested and sectioned for HE staining.

FACS analysis. PiPS and PiPS-EC or control cells and isotype controls were analysed with FACS in order to test the percentage of the KDR and other endothelial and pluripotent markers. Data analysis was carried out using CellQuest software (Becton Dickinson).

In vitro tube formation assay. Cell suspension containing 4×10^4 control or PiPS-ECs were placed on top of the 50 μl/well Matrigel (10 mg/ml; BD Matrigel Basement Membrane Matrix, A6661) in 8-well chamber slides (Nunc). Rearrangement of cells and the formation of capillary-like structures were observed at 18–24 hour.

In vivo angiogenesis assay. PiPS-ECs or control cells were labelled with Molecular Probes Vybrant Cell Labelling (MP22885) before the *in vivo* angiogenesis assay to distinguish the in vitro–differentiated cells from the host cells. PiPS-ECs ($1x10^6$) were mixed with 50 µl of Matrigel and injected subcutaneously into the back or flank of NOD.CB17-*Prkdc*^{scid}/NcrCrl mice. Six injections were conducted for each group. Fourteen days later, the mice were killed and the plugs were harvested, frozen in liquid nitrogen, and cryosectioned. Samples were fixed with 4% paraformaldehyde in PBS at 4°C overnight, and then HE staining was performed. Images were assessed with Axioplan 2 imaging microscope with Plan-NEOFLUAR 10×, NA 0.3, objective lenses, AxioCam camera, and Axiovision software (all Carl Zeiss MicroImaging, Inc.) at room temperature, and were processed with Photoshop software (Adobe).

Lentiviral particle transduction. Lentiviral particles were produced using MISSION shSETSIP plasmids DNA (ShRNA SET TRCN000063717 SIGMA) according to protocol provided and previously described (1). The shRNA Non-Targeting vector was used as a negative control. Briefly, 293T cells were transfected with the lentiviral vector and the packaging plasmids, pCMV-dR8.2 and pCMV-VSV-G (both obtained from Addgene) using Fugene 6. The supernatant containing the lentivirus was harvested 48h later, filtered, aliquoted and stored at –80°C. p24 antigen ELISA (Zeptometrix) was used to determine the viral titre. The Transducing Unit (TU) was calculated using the conversion factor recommended by the manufacturer (10^4 physical particles per pg of p24 and 1 transducing unit per 10^3 physical particles for a VSV-G pseudotyped lentiviral vector), with 1pg of p24 antigen converted to 10 Transducing Units (TU). For lentiviral infection, PiPS-ECs were seeded overnight and the following day the cells were incubated with shSETSIP or Non Targeting control ($1x10^7$TU/ml) in complete medium supplemented with 10µg/ml of Polybrene for 24h. Subsequently, fresh medium was added to the cells and the plates were returned to the incubator and harvested 72h later to be subjected to further analysis.

Luciferase activity assay. VE-Cadherin promoter (2000bp) region was amplified by PCR and cloned into the XhoI/HindIII sites of pGL3-Luc reporter vector, and verified by DNA sequencing. In brief, CTL or PiPS-ECs were transfected with the reporter gene (0.33µg/well) together with expression plasmid (0.16µg/well) encoded from SETSIP, or CTL and PiPS-EC were infected with SETSIP shRNA or CTL shRNA one day before the transfection. pGL3-Luc Renilla (0.1µg/well) was included in all transfection assay as internal control, pCMV5 was also used as mock control. Luciferase and Renilla (Promega) activity assays were detected 48hr after transfection using a standard protocol. Relative luciferase unit (RLU) was defined as the ratio of luciferase activity to Renilla activity with that of control set as 1.0.

Chromatin immunoprecipitation assay. Chromatin immunoprecipitation assay was performed with commercial kit (EZ ChIP, Millipore) according to the protocol provided, and previously described (2). In brief, PiPS-EC and control cells were treated with 1% (vol/vol) formaldehyde at room temperature for 10 min and then quenched with glycine at room temperature. The medium was removed, and cells were harvested in lysis buffer. Following a short incubation on ice, chromatin was sheared by sonication. The sheared samples were diluted into 0.9 ml ChIP Dilution Buffer and precleared with Protein G Agarose/Salmon Sperm DNA beads for 1 h. Subsequently, immunoprecipitation was conducted with similar to SET antibody (sc-5655). Normal IgG was used as a control. Immunocomplexes were collected the following morning using Protein G Agarose/Salmon Sperm DNA beads. Immunoprecipitates were pelleted by centrifugation and washed with Low-Salt Buffer, High-Salt Buffer, and Tris-EDTA buffer (25 mM Tris-HCl, 150 mM NaCl, 1 mM EDTA, pH 7.2) to remove any nonspecific binding. The immunoprecipitates were eluted from the beads using 200 µl of elution buffer (100 mM NaHCO3, 1% SDS**)** and the crosslink of the protein/DNA complexes were reversed by an overnight incubation of the eluted product at 65 °C. A total of 2 µl proteinase K (10 µg/µl) was subsequently added to the solution and samples were incubated at 45 °C for 1 h. DNA was then purified using the spin columns provided. Aliquots of chromatin were also analyzed before immunoprecipitation and served as an input control. VE-cadherin gene promoter sequences were amplified by PCR with primer sets listed in Table S2. The PCR products were analyzed in 2% agarose gel and images were assessed with BioSpectrum AC Imaging System and Vision- WorksLS software.

Nucleofection. Fibroblasts were nucleofected with a polycistronic plasmid (OSKM) containing all four factors (Plasmid 20866: pCAG2LMKOSimO: Sox2, Oct4, Klf4 and cMyc, Addgene), using Amaxa nucleofector (VPD-1001 NHDF Kit, LONZA), and cultured in reprogramming media for 4 days. The 4 day-reprogrammed cells were defined as partial iPS cells (PiPS).

Cell seeding and vascular bioreactor. PiPS-ECs or fibroblasts were seeded on aortic grafts, which were previously decellularized (with sodium dodecyl sulfate (SDS) at 0.075 % and washed in PBS), in a special constructed bioreactor and shear stress was applied. Briefly, a roller pump (Masterflex: Standard Drive, model 7520; Standard Pump Head, model 7018-20; Codane Tubing, Cole-Parmer UK) was used to produce mean flow in the bioreactor, the grafts were fixed between two 25 G needles after hosting them on plastic tubes fixed by 8-0 silk sutures (8-0 black virgin silk, Ethicon Inc., Johnson & Johnson, Norderstedt, Germany). The complete setup was maintained in a standard CO_2 incubator at 37 °C. The scaffolds were placed for the seeding process in a self constructed incubation chamber and preconditioned with cell culture media for 2h. Then, 5 x 10^5 cells of PiPS-ECs or fibroblasts were seeded on the scaffolds via direct injection and allowed to seed for 12h before the initial flow was set up. Decellularized vessels have also been used as a second control. Shear stress was applied at stepwise rates ranging from 10 to 35 dynes/cm^2 over a period of 48h. After this time point no increase in the shear stress rate was conducted and the grafts remained under constant shear stress of 35 dynes/cm^2 until they were harvested by day 4. For the last 24 hours 100 Units of heparin per ml of total circulating reactor media volume (heparin sodium salt diluted, from porcine gastrointestinal mucosa, Sigma Aldrich) was added every 12h. For the double seeded PiPS cells tissue engineering vessels, decellularized vessel scaffolds were placed in a self constructed incubation chamber and preconditioned with differentiation media α-MEM, 10 % FBS and 25 ng/µl PDGF-BB for 2h. After this period 2 x 10^6 PiPS cells were seeded in reprogrammed media via direct injection and allowed to seed for 12h at a continuous rotational movement before initial flow was set up. Shear stress was applied at 10 dynes/sqcm^2 over a period of 48h. Then, the circulating media was exchanged to EGM-2 media and a second seeding step was initiated with 1 x 10^6 PiPS cells and after another 12h seeding period the shear stress rate was stepwise adjusted up to 35 dynes/sqcm^2. The grafts remained under constant shear stress of 35 dynes/sqcm^2 and harvested on day 5. The engineered vessels were harvested and used for further analysis in vitro or immediately grafted to animals.

Ischemia model. The ischemia model was performed as previously described (3). PiPS-ECs were injected intramuscularly into adductors of ischemic SCID mice. Fourteen days later, the hind limb blood flow and muscular neo-angiogenesis were evaluated. The tissue blood flow of both legs was sequentially assessed by a perfusion imager system (Laser Doppler Flow assessment). Hind limb muscles were harvested following in situ perfusion fixation at physiological pressure, frozen in liquid nitrogen, and cryosectioned. Sections of adductor muscles were stained with CD31 antibody and capillary density was expressed as the capillary number per mm^2. Human cell engraftment ability was assessed by counting cells positive for CD31 (human specific antibody) at six randomly selected microscopic fields (at x100).

En face **preparation and immunofluoresence staining and frozen section staining**. The procedure for en face preparation is similar to that described elsewhere (4). In short, the tissue-engineered vessels or grafts were harvested, and the samples were fixed with acetone and cut open. The vessel segments were mounted and pinned onto rubber with the lumen opened and facing up. After washing with PBS specimens were placed in a humidified chamber and blocked in 5% swine serum in PBS for 30 min at 37˚C and incubated with primary antibodies rabbit anti-VE-cadherin, and rabbit anti-CD31 as described in the immunostaining section above. For frozen section staining, serial 5 mym-thick frozen sections were cut from cryopreserved tissue blocks, fixed in a cold 1:1 acetone 10 minutes, and washed with phosphate-buffered saline (PBS) for 20 minutes, and proceed as described above.

Miller's elastin staining. To assess the elastic lamina in the tissue-engineered vessel sections, the Miller's elastin staining was applied. In brief, paraffin sections were deparaffinised and rehydrated. They were then immersed in potassium permanganate, then oxalic acid and finally rinsed in 70% ethanol. The tissue was incubated in Miller's elastin stain (BDH Laboratory Supplies, Poole UK) for 3 hrs followed by counterstaining with van Gieson solution (50% saturated picric acid solution, 0.09% acid fuchsin) for 5 min. Sections were subsequently dried, dehydrated and mounted on microscope slides. Staining was visualized as described above.

SI References

1. Margariti A, et al. (2010) Histone deacetylase 7 controls endothelial cell growth through modulation of beta-catenin. *Circ Res* 106:1202-1211.
2. Margariti A, et al. (2009) Splicing of HDAC7 modulates the SRF-myocardin complex during stem-cell differentiation towards smooth muscle cells. *J Cell Sci* 122:460-470.
3. Emanueli C, et al. (2007) Nitropravastatin stimulates reparative neovascularisation and improves recovery from limb Ischaemia in type-1 diabetic mice. *Br J Pharmacol* 150:873-882.
4. Zeng L, et al. (2009) Sustained activation of XBP1 splicing leads to endothelial apoptosis and atherosclerosis development in response to disturbed flow. *Proc Natl Acad Sci U S A* 106:8326-8331.

Table S1. Primers

Name	Sequence	NCBI Reference Sequence
PHEX	5'>ACAACTTTGCTGCCTCAATGGGAC<3' 5'>TCGTTCCTGCATCCATCCACTCAT<3'	NM_000444.4
DMP1	5'>TGGAGATGACACCTTTGGTGACGA<3' 5'>TGGTGGTATCTTGGGCACTGTCTT<3'	NM_001079911.2
ADIPOQ	5'>ATCCAAGGCAGGAAAGGAGAACCT<3' 5'>TGGTAAAGCGAATGGGCATGTTGG<3'	NM_001177800.1
Adipsin	5'>TGATGTGCGCGGAGAGCAAT<3' 5'>TAGATCCCGGGCTTCTTGCGGTT<3'	NM_001928.2
ACVR1C	5'>TGGTTTACTGGGAAATAGCCCGGA<3' 5'>CACAACTTTGCCACTGGTTTGGGA<3'	NM_001111031.1
NRARP	5'>GCTGTGCGCAAGGGCAACAC<3' 5'>GAACGCGGCGATGTGCAGC<3'	NM_001004354.1
Filamin	5'>CCACCGGCACTGTCCTTCGC<3' 5'>AGCCACTGCCCTCAGCCCTT<3'	NM_015687.2
LIM2	5'>GCGCCTGGGGAAAGAGCAGG<3' 5'>AAGCGCCAGTCCCCAAAGCG<3'	NM_030657.3
LSS	5'>ATGCAGGGCACCAACGGCTC<3' 5'>CAGCTCCAGCAAGTGCCCCC<3'	NM_002340.5
TEK	5'>TGCATTGCCTCTGGGTGGCG<3' 5'>AGCCTGGTGAAGGCCGAGGT<3'	NM_000459.3
SPRY	5'>GCCAGCCTCCGGCAATTCCT<3' 5'>CCTCGCCCTCCTTTCGCAGC<3'	NM_032681.3
STMN2	5'>CGTGCCTCTGGCCAGGCTTT<3' 5'>CTGCGCACCTCCGCAGCAT<3'	NM_007029.2
HBA2	5'>ACGCTGGCGAGTATGGTGCG<3' 5'>GGTCACCAGCAGGCAGTGGC<3'	NM_000517.4
DNMT3L	5'>TGTGTACGGCGCCACACCTC<3' 5'>CAGAGCCCAGTGCCTGCTGC<3'	NM_013369.2
ARRDC4	5'>GGCTGCTATTCCAGCGGCGA<3' 5'>CAGGCTGAGGCGCACGTTCA<3'	NM_183376.2
Oct-01	5'>GCCTCAGCCTCCACCTCCGA<3' 5'>AGGCACCTCCAGCCGCAAAC<3'	NM_002697.2
TNC	5'>AGGCCGGTGCATTGATGGGC<3' 5'>CAGGCATGTGGGCAGGTGGG<3'	NM_002160.2
C-KIT	5'>TGAATGGCATGCTCCAATGTGTGG<3' 5'>ACATCCACTGGCAGTACAGAAGCA<3'	NM_000222
CD133	5'>TACCAAGGACAAGGCGTTCACAGA<3' 5'>GTGCAAGCTCTTCAAGGTGCTGTT<3'	NM_001145847
CD34	5'>CACTGAGCAAGATGTTGCAAGCCA<3' 5'>TCAGGAAATAGCCAGTGATGCCCA<3'	NM_001025109
KDR	5'>ATCCAGTGGGCTGATGACCAAGAA<3' 5'>ACCAGAGATTCCATGCCACTTCCA<3'	NM_002253

OCT4	5'>ATGCATTCAAACTGAGGTGCCTGC<3'	NM_001173531
	5'>AACTTCACCTTCCCTCCAACCAGT<3'	
SOX2	5'>CACATGAAGGAGCACCCGGATTAT<3'	NM_003106
	5'>GTTCATGTGCGCGTAACTGTCCAT<3'	
KLF4	5'>TGACCAGGCACTACCGTAAACACA<3'	NM_004235
	5'>TCTTCATGTGTAAGGCGAGGTGGT<3'	
c-MYC	5'>ACAGCTACGGAACTCTTGTGCGTA<3'	NM_002467
	5'>GCCCAAAGTCCAATTTGAGGCAGT<3'	
SETSIP-LOC646817	5'>ATGGTCTGGTTCTTGGACTTCCCT<3'	XM_929774
	5'>AGCAGGAGGTGGTCTTGGTTTCTT<3'	
CD31	5'>GAACAGGACCGCGTTTTATCC<3'	NM_000442.4
	5'>ATTCCGTCACGGTGACCAGTT<3'	
eNOS	5'>TGATGGCGAAGCGAGTGAA<3'	NM_000603.4
	5'>ACTCATCCATACACAGGACCCG<3'	
vWF	5'>TGCGAAGTACCTTGGTTACCCA<3'	NM_000552.3
	5'>TAATCGTCAGTACATGCCCCG<3'	
CD144	5'>ATGAGAATGACAATGCCCCG<3'	NM_001795
	5'>TGTCTATTGCGGAGATCTGCAG<3'	
SETSIP-LOC646817	5'>CGGTGCGGTACCCTCATGGTCTGGTTCTTG>3'	SETSIP CLONING
	5'>CGTAGCTCTAGAGTCATCTTCTCCTTCATC>3'	
VE-Cadherin Promoter	5'>CCTGAGACAGAGGAATCACTATCC>3'	864-1152 bp
	5'>CAGGAGAGACATAGGAGGAGCTT>3'	

Table S2. Gene regulations at day 4.

	Upregulated	**Downregulated**
Genes involved in Differentiation	BHLHB2	CCL2
	CCND2	CEBPD
	EGR1	CTSB
	EGR2	CXCL12
	ENC1	DCN
	FABP5	EPAS1
	ID1	FAM2OC
	IGF2	GAS1
	IGFBP3	HSPA2
	IGFBP5	IL6
	IRF7	IL8
	LRRC17	LAMA4
	PNP	MMP1
	POU5F1	NFKBIA
	RGS2	PDK4
	TIMP3	SFRP1
	VCAM	SOD2
		TCF21
		TNC
		TNFRSF11B
		TNFRSF12A
		TWIST2
Differentiation of Connective tissue	LRRC17	CCL2
	POU5F1	IL6
	RGS2	IL8
	TIMP3	LAMA4
		MMP1
		SFRP1
		SOD2
		TNFRSF11B
		TWIST2
Differentiation of muscle cell lines	IGF2	CTSB
	IGFBP5	CXCL12
	TNFRSF12A	DCN
		TCF21
Differentiation of adipocytes	RGS2	IL6
	TIMP3	LAMA4

		MMP1
		SFRP1
		SOD2
Differentiation of bone cell lines	BHLHB2	CXCL12
	CCND2	IL6
	EGR1	
	RGS2	
Differentiation of mononuclear cells		CCL2
		IL8
Differentiation of oesteoclast-like cells	IGF2	CCL2
		IL8
		CXCL12
		IL6
		MMP1
		TNFRSF11B
Formation of endothelial tube	KLF2	CCL2
		CXCL12
		IL8
Adhesion of endothelial cells	EGR1	CCL2
	SERPINE1	CXCL12
	VCAN	DCN
		IL6

Genes changed during cell reprogramming are involved in cell differentiation into distinct cell lineages at day 4 of reprogramming. Data was analyzed using the Ingenuity Systems Software.

Table S3. Gene regulations at day 7

	Upregulated	Downregulated
Differentiation of memory B cells		BCL6 IL6
Differentiation of β lympocytes	SYK	BCL6 EGR1 IL6
Differentiation of Th2 cells	LL13RA2	BCL6 IL6
Differentiation of Osteoclast Precursor cells	IL32	IL6

Genes changed during cell reprogramming are involved in cell differentiation into distinct cell lineages at day 7 of reprogramming. Data was analyzed using the Ingenuity Systems Software.

Table S4. Gene regulations at day 14

	Upregulated	**Downregulated**
Genes involved in Differentiation	HES5	BCL6
	IGFBP6	BDNF
	IL8	EGR1
	IL13RA2	ETS1
	MMP3	IGFBP3
	POU5F1	IL6
	STMN2	INSIG1
		NR4A2
		TSC22D3
Differentiation of stem cells	POU5F1	BDNF
		IL6
		NR4A2
		TSC22D3
Differentiation of Th17 cells		BCL6
		ETS1
		IL6
Differentiation of Dopaminergic neurons		BDNF
		NRYA2
Differentiation of memory B cells		BCL6
		IL6
Differentiation of Th2 cells		BCL6
		IL6
		IL13RA2
Differentiation of helper T lymphocytes	IL13RA2	BCL6
		ETS1
		IL6
Differentiation of Embryonic cells		BDNF
		IL6
		NR4A2
		POU5F1
Differentiation of central nervous system	IGFBP6	BDNF
		HES5
Differentiation of lymphoblastoid cell lines		IL6
Differentiation of mesenchymal stem cells		BDNF
		TSC22D3
Differentiation of plasma cells		BCL6
		IL6

Table S5. Gene regulations at day 21

	Upregulated	Downregulated
Genes involved in differentiation	CD44	BCL6
	DCN	EGR1
	FES	ETS1
	IGFBP6	INS1G1
	IL8	TNC
	IL32	TSC22D3
	IL1B	
	INSM1	
	KRT8	
	MAFB	
	MMP3	
	MMP1	
	POU5F1	
	S100A4	
	SERPINB2	
	STC1	
	SYK	
Differentiation of Endothelial progenitors	IL1β	IGFBP3
Differentiation of connective tissue cells	IL8	INSIG1
	IL32	
	IL18	
	MMP3	
	MMP1	
	POU5F1	
	STC1	
Differentiation of Th17 cells	IL1β	BCL6
		ETS1
Differentiation of Oligodendrocytes		HES5
		IL1β
Tubulation of Endothelial cell lines	FES	TGFβ1
	IL8	

Genes changed during cell reprogramming are involved in cell differentiation into distinct cell lineages at day 21 of reprogramming. Data was analyzed using the Ingenuity Systems Software.

Supplemental Figures

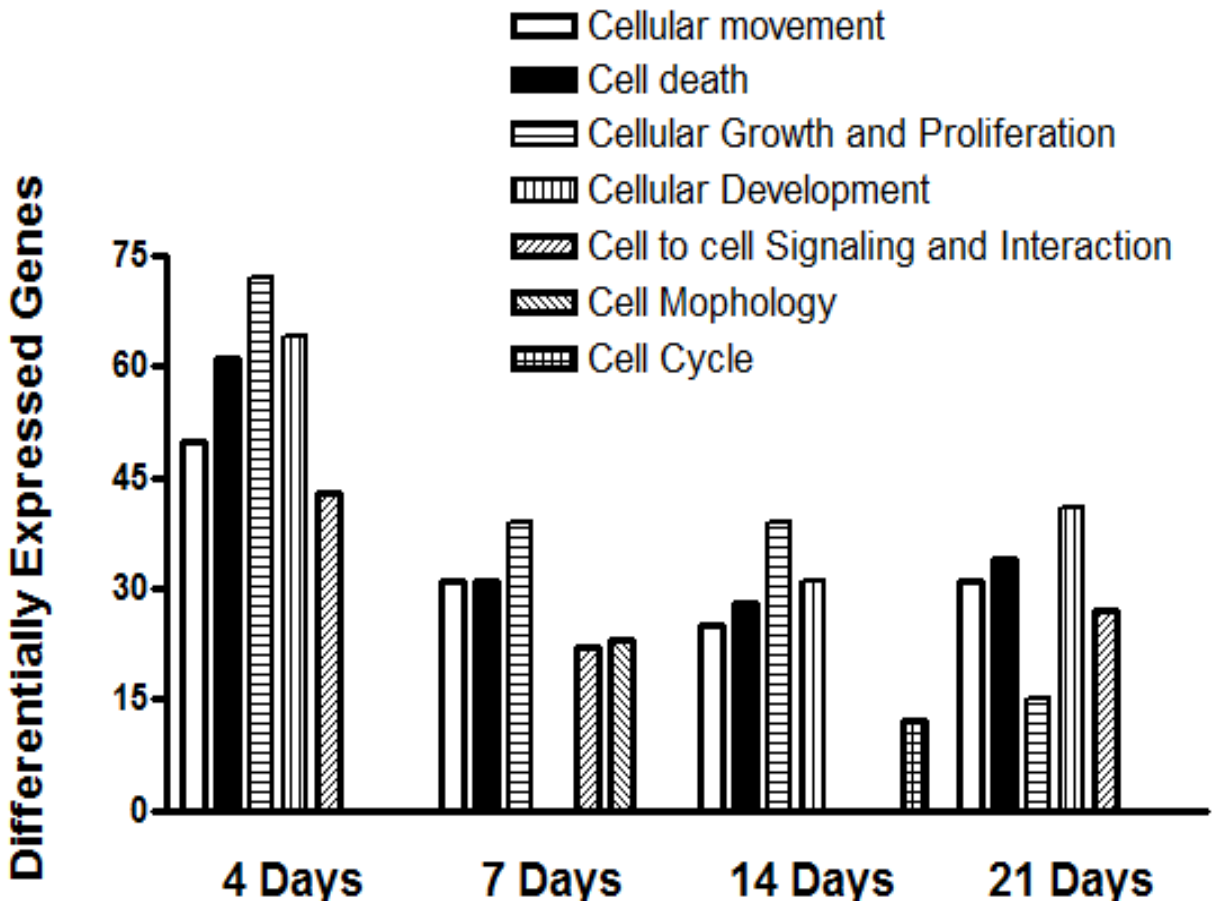

Fig. S1. Functional Classification. Human fibroblasts were virally transduced with a plasmid encoding the four transcription factors OCT4, SOX2, KLF4, c-MYC and cultured in reprogramming media**.** Microarray analysis was performed at days 4, 7, 14 and 21, and functional classification of the genes altered were analysed using the Ingenuity Systems Software.

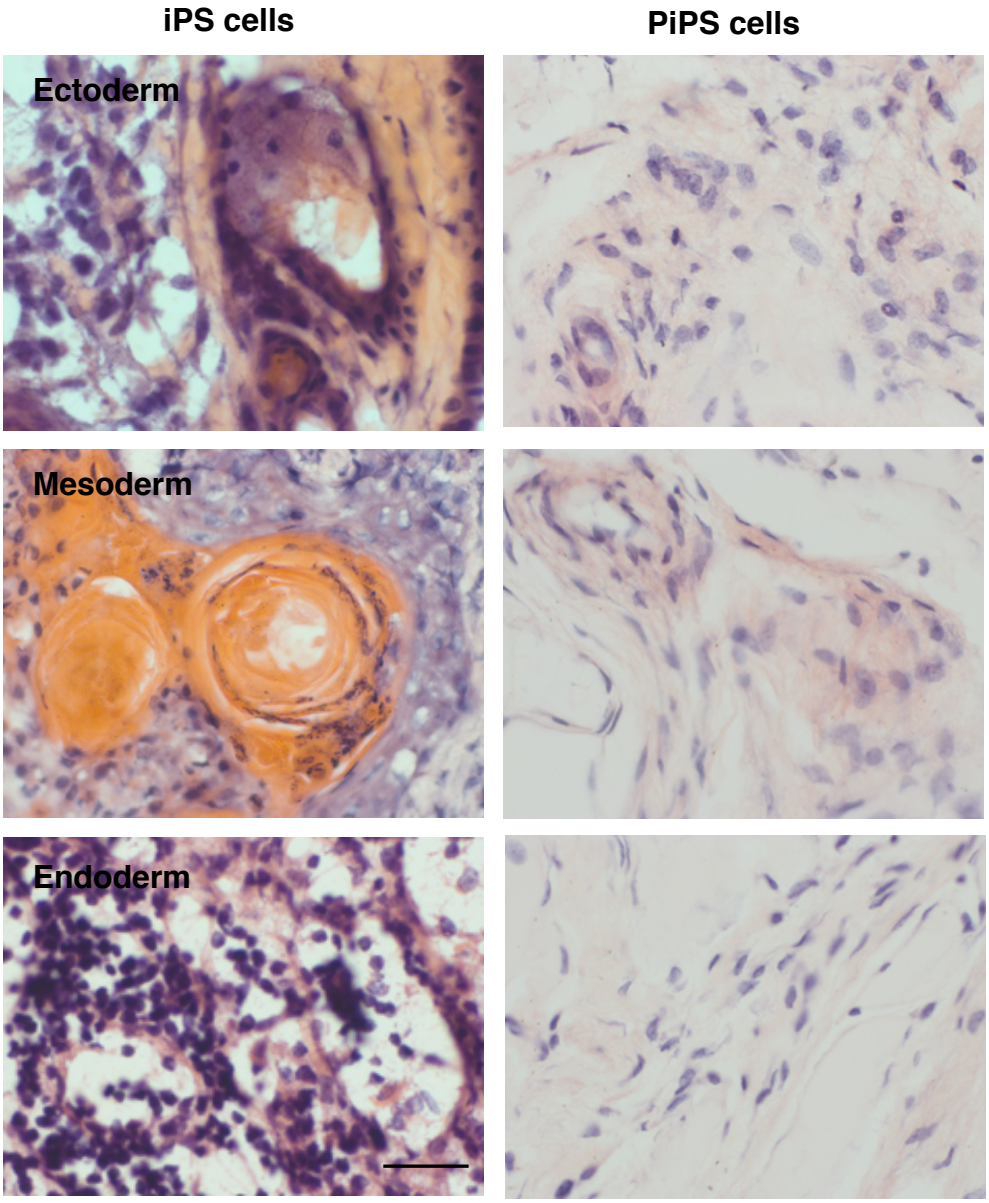

Fig. S2. Immunodeficient mouse recipients (SCID) were subcutaneously injected with human iPS cells or human PiPS cells for a Matrigel plug. Eight weeks later, the plugs were harvested, sectioned and stained with HE. Note that teratoma formation was observed in iPS cells but not in PiPS cells. iPS cells resulting teratomas demonstrate features in ectoderm, mesoderm, and endoderm (left panel). In contrast, an amorphous cellular mass was observed in PiPS cell matrigel plugs (right panel). Scale bar, 50 μm.

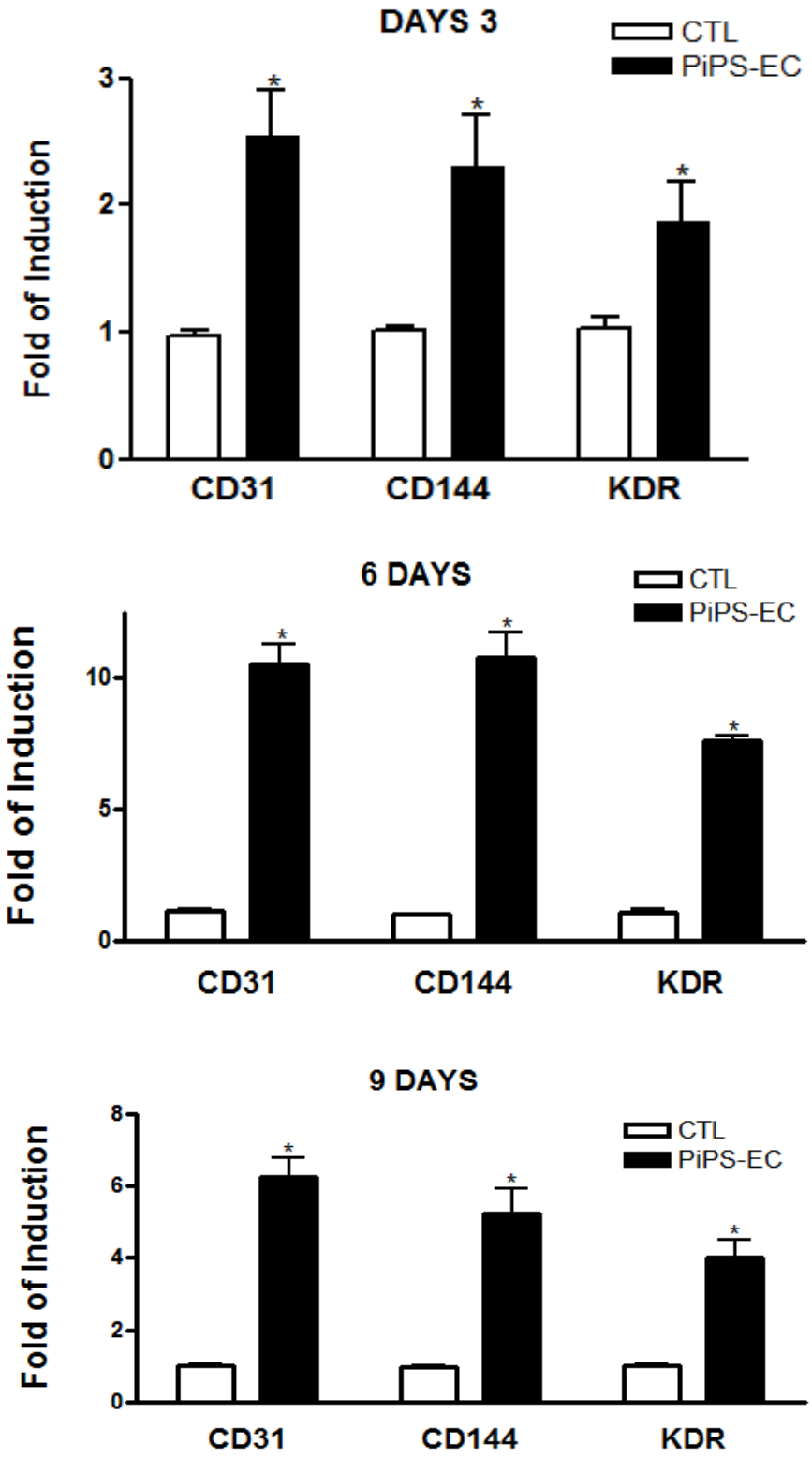

Fig. S3. Time-course of PiPS cells differentiate into endothelial cells. PiPS or control cells were seeded on collagen IV-coated plates and cultured with EGM-2 media for 3-9 days. PiPS-ECs expressed endothelial markers CD31, CD144, and KDR, (data are means ± SEM. (n=3), *p<0.05)

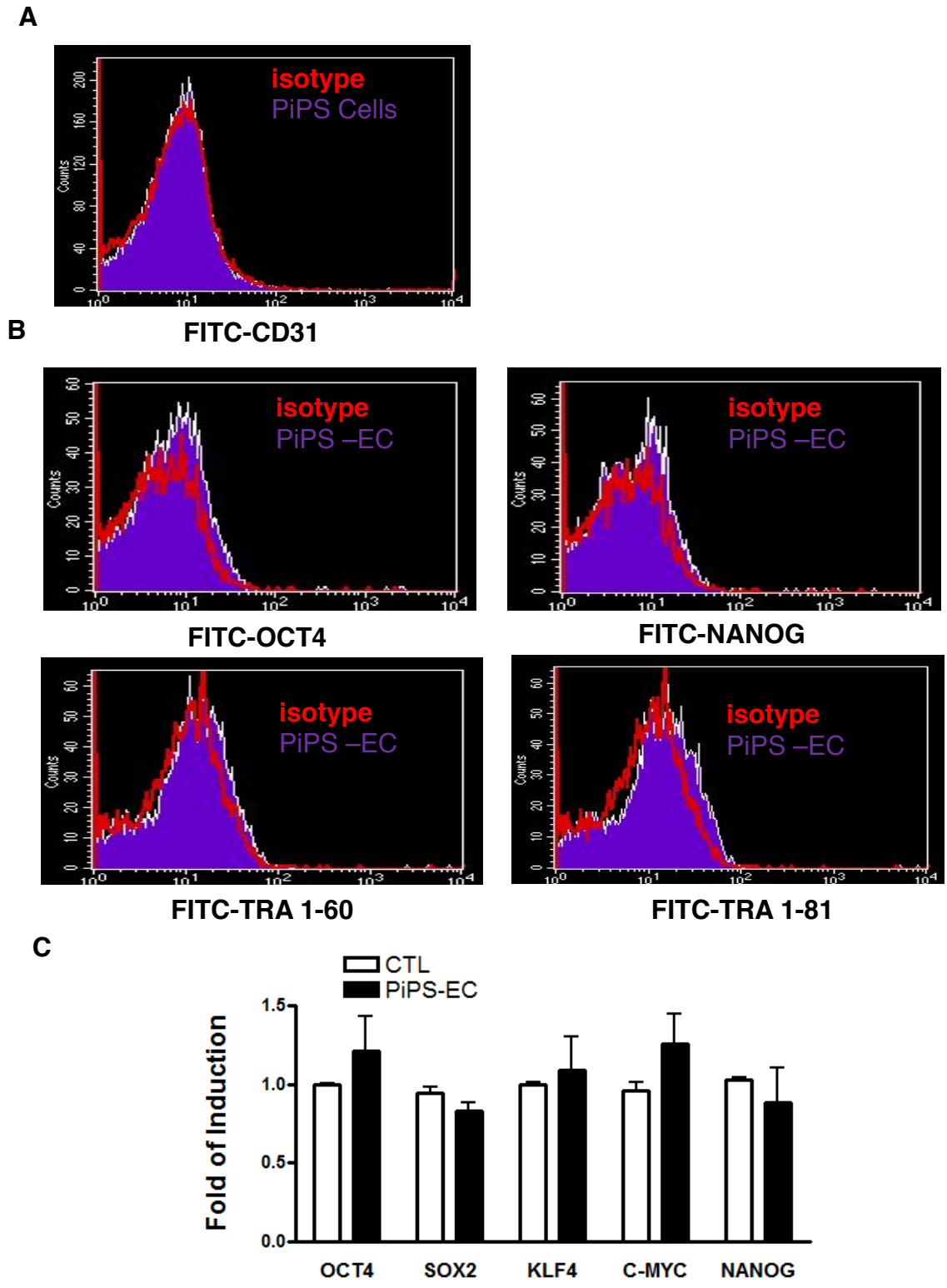

Fig. S4. PiPS-ECs did not express pluripotent markers. (A) FACS analysis for Undifferentiated PiPS cells with CD31. (B) PiPS-ECs for pluripotent markers, OCT4, NANOG, TRA1-60, TRA1-81, and isotype controls. (C) Real time PCR for OCT4, SOX2, KLF4, C-MYC, and NANOG for PiPS-ECs, (data are means ± SEM. (n=3).

A

PREDICTED: Homo sapiens similar to SET (LOC646817), mRNA.

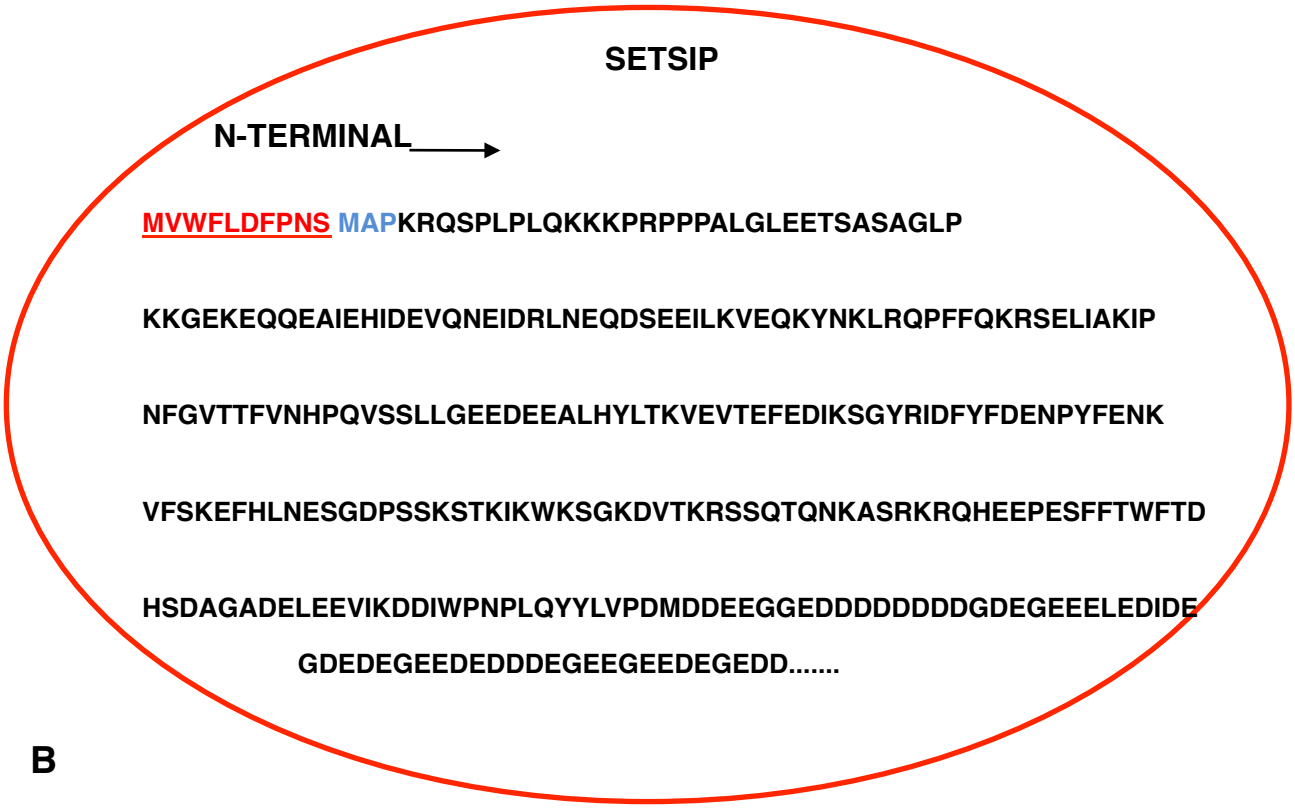

B

Homo sapiens SET nuclear (SET), transcript variant 1, mRNA.

N-TERMINAL ⟶

MAPKRQSPLPPQKKKPRPPPALGPEETSASAGLPKKGEKEQQEA
IEHIDEVQNEIDRLNEQASEEILKVEQKYNKLRQPFFQKRSELIAKIPNFWVTTFVNH
PQVSALLGEEDEEALHYLTRVEVTEFEDIKSGYRIDFYFDENPYFENKVLSKEFHLNE
SGDPSSKSTEIKWKSGKDLTKRSSQTQNKASRKRQHEEPESFFTWFTDHSDAGADELG
EVIKDDIWPNPLQYYLVPDMDDEEGEGEEDDDDEEEEGLEDIDEEGDEDEGEEDEDD
DEGEEGEEDEGEDD .....

Fig. S5. A gene defined as a similar to SET protein (SETSIP-LOC646817), was identified by microarray analysis. SETSIP gives rise to a protein containing 10 additional amino acids in the N-terminal (A) in comparison to the known SET protein (B).

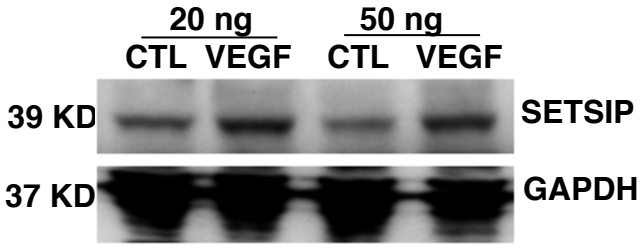

Fig. S6. VEGF induced SETSIP expression in protein level. PiPS-ECs were subjected to further treatment with 20ng/ml and 50 ng/ml of VEGF and the expression levels of SETSIP were detected.

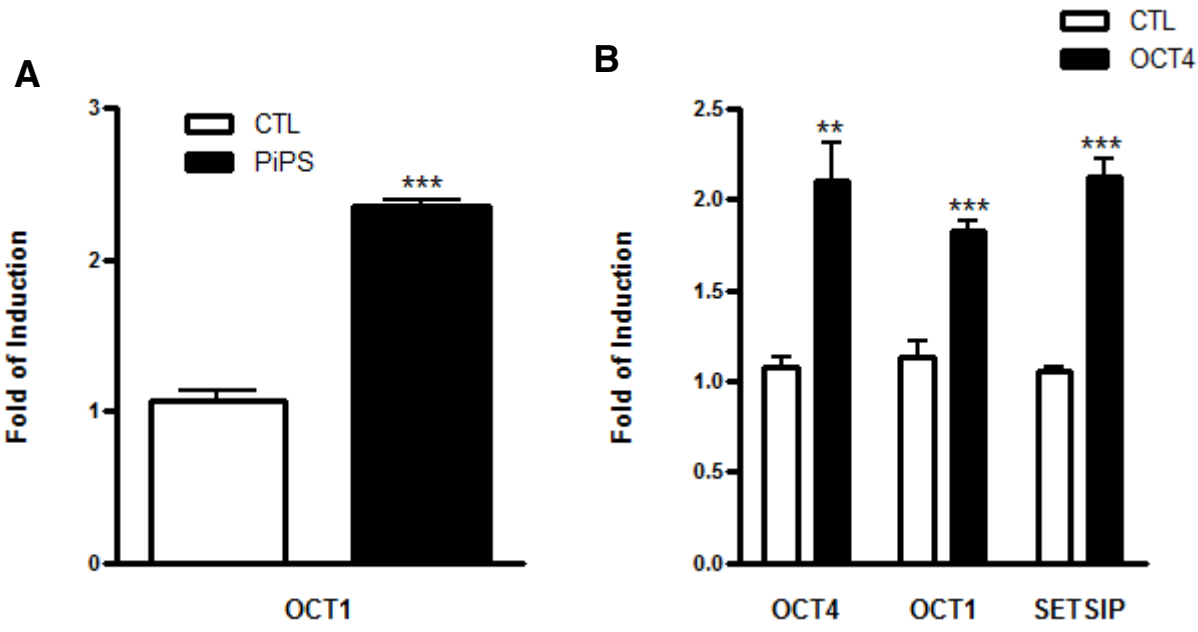

Fig. S7. OCT1 expression is induced during stages of reprogramming (data are means ± SEM (n=3), ***p<0.001) (A), while overexpression of OCT4 in fibroblasts resulted in OCT1 and SETSIP activation (data are means ± SEM (n=3), **p<0.01, ***p<0.001) (B).

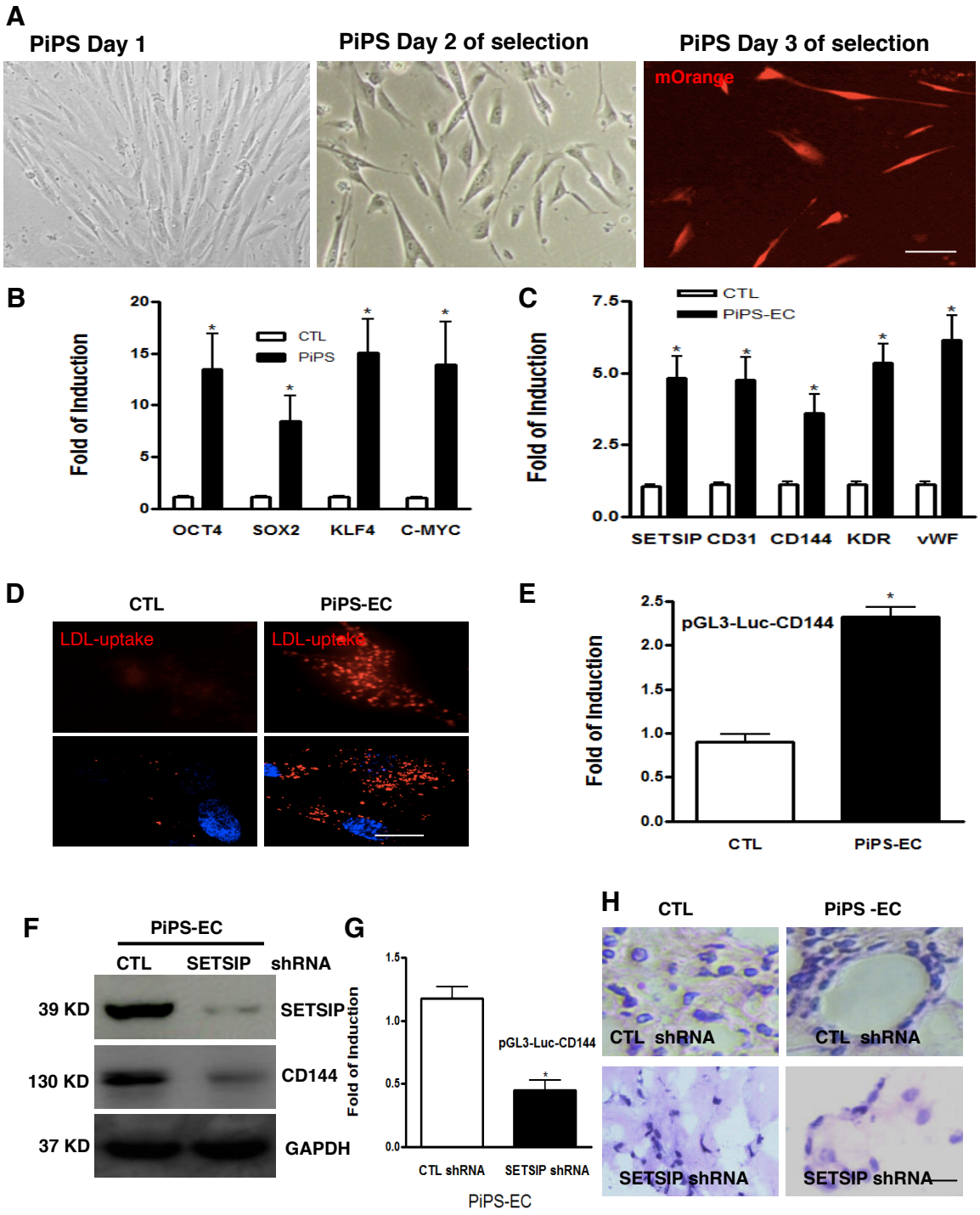

Fig. S8. A pure population of PiPS cells was selected with neomycin and differentiated into EC cells. (A) Images show one day (left panel) nucleofected human fibroblasts with a pCAG2LMKOSimO plasmid encoded the four reprogrammed factors (OCT4, SOX2, KLF4 and c-MYC), which also contains a neomycin registrant gene and a mOrange marker. Selection of PiPS cells with neomycin has started one day after the transfection and images show 2 days PiPS cells after selection (middle panel) and mOrange expression at 3 days of selection (right panel). (B) The selected PiPS cells express the four reprogrammed factors at mRNA levels (data are means ± SEM. (n=3), *p<0.05). (C) Real time PCR assay shows that the selected PiPS cells differentiate into ECs (data are means ± SEM. (n=3), *p<0.05). (D) PiPS-EC cells display the capacity of LDL uptake. Scale bar, 50 µm. (Upper panel; live image, lower panel; cells were fixed and 4',6-diamidino-2-phenylindole DAPI was used and stained the cell nucleus). (E) Luciferase assays demonstrate an increased promoter activity of VE-cadherin in PiPS-EC derived from a pure population of PiPS cells in comparison to the control cells (data are means ± SEM. (n=3), *p<0.05). (F) Knockdown of SETSIP by shRNA in PiPS-ECs resulting in suppression of VE-cadherin in the protein level. (G) Luciferase assays demonstrate a decrease in the promoter activity of VE-cadherin after knockdown of SETSIP by shRNA in PiPS-ECs (data are means ± SEM. (n=3), *p<0.05). (H) The formation of vascular-like tubes *in vivo* in Matrigel plugs is abolished by knockdown of SETSIP using shRNA. Scale bar, 50 µm.

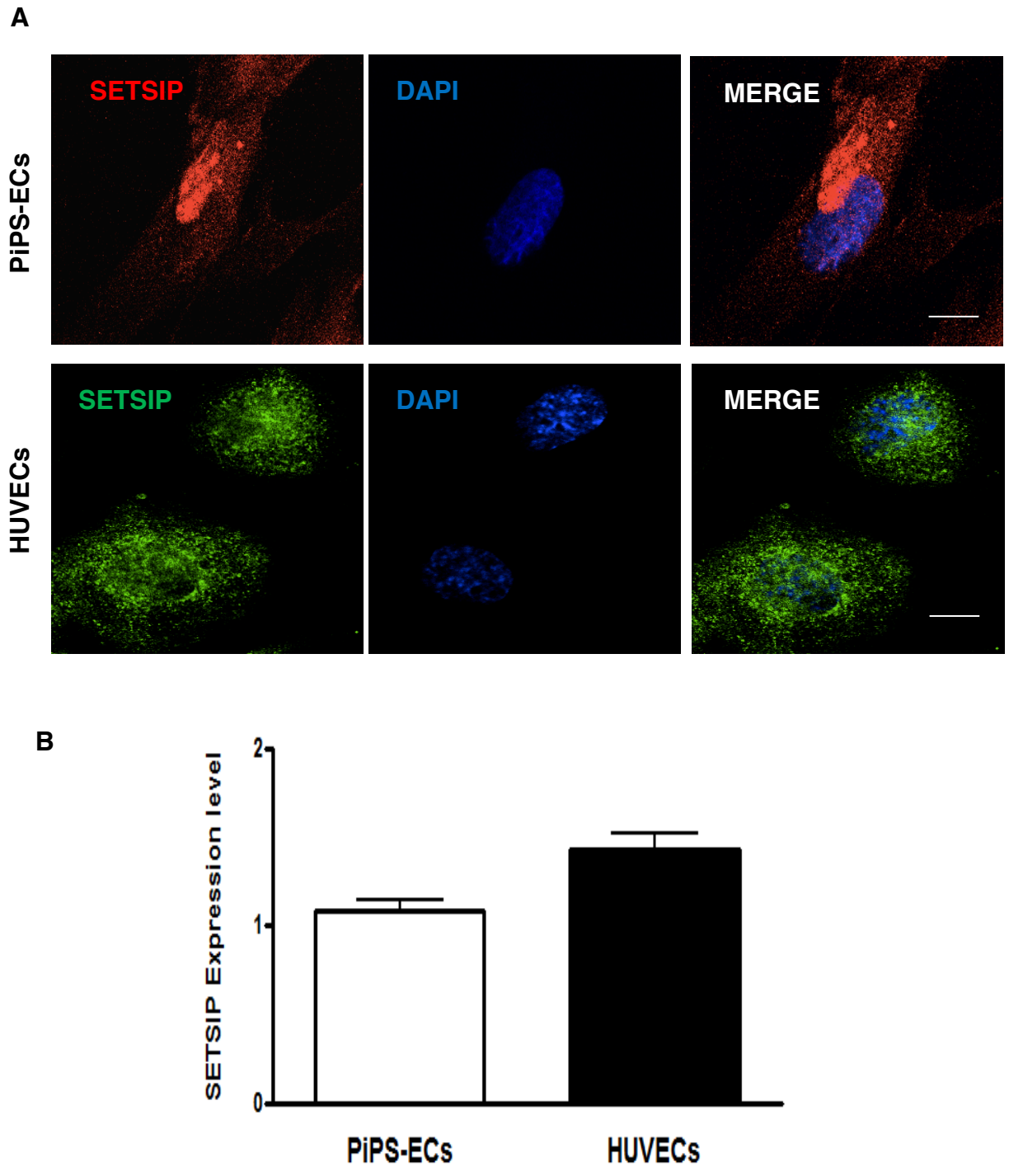

Fig. S9. SETSIP is expressed in PiPS-ECs and mature ECs. Mature ECs were isolated from human umbilical cord (HUVECs). (A) Immunostaining shows SETSIP nuclear localization in both PiPS-ECs and HUVECs, Scale bar, 50 μm. (B) Real-time PCR data for SETSIP mRNA expression in PiPS-ECs and HUVECs (data are means ± SEM (n=3)).

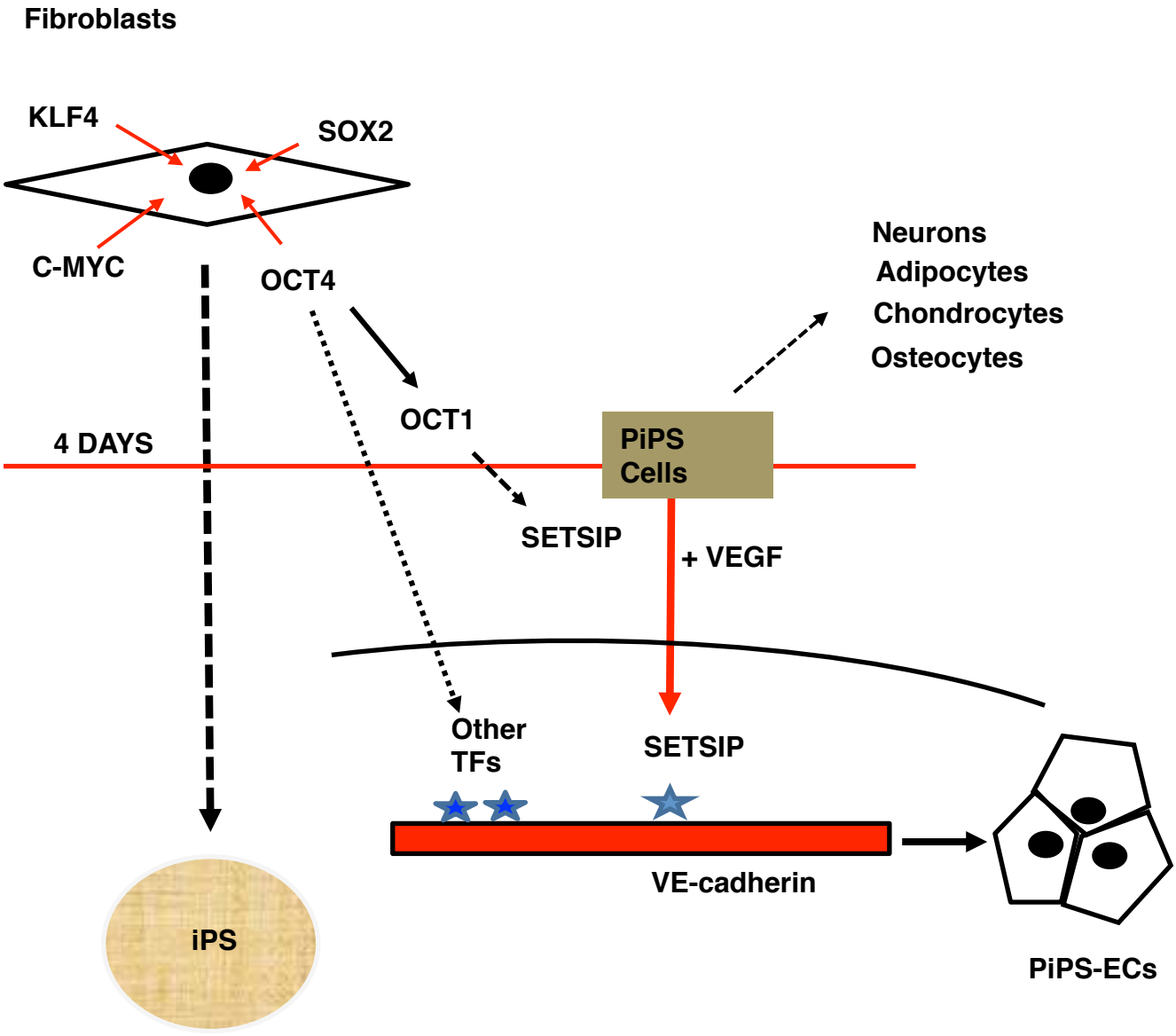

Fig. S10. Schematic diagram showing that short term reprogramming of fibroblasts with four factors generated Partial-iPS (PiPS) cells, which displayed the potential to differentiate into functionally ECs via OCT4-SETSIP and VEGF signal pathways. Preliminary data also showed that PiPS cells in response to defined media and culture conditions induced the expression of markers of other cell lineages, such as neurons, adipocytes, osteocytes, chondrocytes.